Reprinted from JOURNAL OF THE ATMOSPHERIC SCIENCES, Vol. 50, No. 18, 15 September 1993
American Meteorological Society

A Fourier–Riccati Approach to Radiative Transfer. Part I: Foundations

P. M. GABRIEL, S.-C. TSAY,* AND G. L. STEPHENS

Colorado State University, Fort Collins, Colorado

(Manuscript received 9 October 1992, in final form 22 February 1993)

ABSTRACT

The three-dimensional equation of radiative transfer is formally solved using a Fourier–Riccati approach while calculations are performed on cloudy media embedded in a two-dimensional space. An extension to Stephens' work, this study addresses the coupling between space and angle asserted by the equation of transfer. In particular, the accuracy of the computed radiation field as it is influenced by the angular resolution of the phase function and spatial discretization of the cloudy medium is discussed. The necessity of using a large number of quadrature points to calculate fluxes even when the phase function is isotropic for media exhibiting vertical and horizontal inhomogeneities is demonstrated. Effects of incorrect spatial sampling on both radiance and flux fields are also quantified by example. Radiance and flux comparisons obtained by the Fourier–Riccati model and the independent pixel approximation for inhomogeneous cloudy media illustrate the inadequacy of the latter even for tenuous clouds.

1. Introduction

Radiative transport is intimately connected with numerous important climatological processes. It is therefore reasonable to suppose that better understanding of these processes can be attained by a more accurate treatment of cloud–radiation interactions. Although it is evident that clouds are inhomogeneous structures, little attention has been paid to the effects exerted by cloud microstructure on the radiation field (cf. Lovejoy et al. 1990 and references therein). Hence, it is expected that inadequate treatment of cloud microstructure must introduce errors in the computed radiances whose magnitudes cannot be known nor are easily estimable and can lead to paradoxes such as the albedo paradox (Wiscombe 1984). The problem is complex, involving in the general case the solution of the three-dimensional radiative transfer equation (RTE).

To simplify the problem, often the effects of horizontal inhomogeneity are artificially introduced by either subdividing a region of space into areas, each assumed uniform and over which plane-parallel theory is assumed locally applicable (the so-called independent pixel approximation), or through the related notion of a cloud fraction. The latter implies that cloud and radiance fields are uncorrelated (Stephens 1988). Conversely, the "averaged" optical properties of naturally occurring clouds, such as their phase function or optical depth, are often derived by associating radiances exiting plane-parallel slabs to these optical properties as if the correspondence was one to one. Although abundant evidence exists attesting to the nonuniformity of clouds (King et al. 1981; Lovejoy 1982; Derr and Gunter 1982; Tsay and Jayaweera 1984; Rhys and Waldvogel 1986; Kuo et al. 1988; Welch et al. 1988a,b; Cahalan and Joseph 1989; Yano and Takeuch 1990) and radiation (Cahalan 1989; Weilicki and Welch 1986; Gabriel and Lovejoy 1988), the continuing use of plane-parallel theory is probably rooted in the hope that over sufficiently large spatial scales clouds have a plane-parallel character or equivalently, that the effects of horizontal structures present in clouds are unimportant.

This paper presents a method of solution of the RTE that allows for the investigation of the relationship between spatial sampling of the cloudy medium and the emerging radiances and the angular resolution required of these radiances to accurately calculate the flux fields. While there are several works detailing how to solve the two- and three-dimensional RTE (most of these are summarized in Table 1), the important spatio–angular coupling implied by the transfer equation has not received adequate attention. To address this problem, a spectral model of the RTE has been formulated and implemented. Known herein as the Fourier–Riccati model, it is representative of a large class of spectral models and is an extension of the work by Stephens (1986).

The orientation of this work is pedagogical. Clouds are characterized by spatially continuous, periodic ex-

* Current affiliation: Goddard Space Flight Center, Greenbelt, Maryland.

Corresponding author address: Dr. P. M. Gabriel, Department of Atmospheric Sciences, Colorado State University, Fort Collins, CO 80523.

TABLE 1. Literature survey of techniques used to solve the two- and three-dimensional radiative transfer equation. This survey extends from 1975 to 1992.

Year	Reference	Physical situation	Method of solution
1975, 1978	Romanova	Uniform illumination of a periodic cloud at its upper boundary. Harmonic extinction, scattering functions of the form: $\alpha = \alpha_0(1 + \epsilon \cos(\omega x))$ and $s = s_0(1 + \epsilon \cos(\omega x))$.	Perturbation series expansion of the radiance. Elements of series decomposed by Fourier expansion. Analytic expressions for single scattering and for the radiance are found in the small-angle approximation associated with a strongly forward-peaked phase function. The 1978 paper provides some numerical results.
1976	Romanova	Uniform illumination of a periodic cloud at its upper boundary. Extinction and scattering functions are expressed as a Fourier series.	Use of invariance principles to formulate expressions for scattering and transmission operators. Medium assumes only horizontal inhomogeneities.
1981	Romanova and Tarabukhina	See 1976 reference.	As in 1976 reference. Numerical solutions obtained for isotropic phase functions in semi-infinite atmospheres over a range of single scattering albedos.
1983	Mironova	See 1976 reference.	As in 1976 reference. This paper is a correction to the 1975 paper of Romanova. Numerical results are provided for phase functions associated with various monodispersions.
1984a, b	Diner and Martonchik	Uniform illumination of a periodic, three-dimensional, vertically nonuniform atmosphere bounded by a reflecting, nonuniform surface.	Transformation of three-dimensional equation of transfer to a system of one-dimensional transfer equations using Fourier transform technique. Numerical results obtained by Gauss–Seidel iterations.
1985	Diner and Martonchik	As in 1984a,b reference.	Interaction principle used to develop adding and doubling technique for numerically solving the one-dimensional transfer equation in 1984a,b references.
1985	Romanova	See 1976 reference. The possibility of gaseous absorption is allowed provided that the volume absorption coefficient is uniform within the cloud layer and that the transmission function of the gas can be approximated by exponential sum fitting. A method is developed to calculate the spatially averaged absorption without requiring the spatially averaged albedo or transmission.	Perturbation method as in 1975 paper. Spatially averaged quantities are obtained via a Fourier transform technique. Phase functions are approximated by the delta-Eddington method.
1986	Stephens	Uniform illumination of a two-horizontally inhomogeneous cloud subject to periodic boundary conditions.	Media is assumed vertically uniform. Two-dimensional transfer equation is Fourier-transformed into a one-dimensional system of ordinary differential equations. A doubling method is used to calculate the radiances. Use of the interaction principle leads to a global response operators defined by a system of nonlinear matrix initial value problems.
1988	Stephens	See 1986 reference.	A formulation of the RTE based on scale hierarchy and closure is presented that provides a means for studying the effects of spatial inhomogeneity and scale interactions on the radiative transfer.
1989	Calahan	Fractal clouds characterized by a single parameter with periodic and open boundary conditions subject to uniform/slant illumination on the upper boundary.	Monte Carlo simulations and independent pixel approximations.
1990a	Lovejoy et al.	This paper develops discrete angle radiative transfer theory for fractal and homogeneous clouds.	See 1990b, 1990c.
1990b	Gabriel et al.	Fractal clouds with normal illumination subject to periodic and open boundary conditions. Conservative scattering was assumed.	Renormalization of the discrete angle equations used to obtain a power law behavior of domain-averaged albedo in the thick cloud limit.

TABLE 1. (*Continued*)

Year	Reference	Physical situation	Method of solution
1990c	Davis et al.	See Gabriel 1990b.	Discrete angle radiative transfer equations were solved using relaxation methods to obtain the radiances inside a fractal lattice. Fluxes were also obtained using forward Monte Carlo simulations.
1991	Kobayashi	See Stephens 1986.	This work follows the methodology of Stephens' 1986 paper. Unlike in Stephens, the solar zenith angle is not a quadrature angle and the solution is determined by the discrete ordinates method.
1991	Davis et al.	A multifractal cloud model was investigated numerically for various mean optical depths. Periodic boundary conditions were applied.	Forward Monte Carlo simulations were applied to obtain all internal and exiting radiative fields in a discrete angle approximation. The discrete angle radiative transfer equations were also solved by using relaxation techniques.
1992	O'Brien	See Stephens 1986.	Backwards Monte Carlo technique solves equation of transfer by a Neumann series. The high-order integrals are efficiently calculated by sampling the integrand using a Hammersley–Halton point sequence. Convergence of the integrals is further promoted by transforming path integrals to transmission integrals, scattering integrals from angle to fraction of phase function integrals.
1992	Evans	Radiative transfer in general media subject to periodic boundary conditions. Media embedded in two dimensions.	The spherical harmonic spatial grid method is an efficient numerical technique for calculating radiances and fluxes in media embedded in two dimensions. This method exploits the smooth angular dependence of the radiance fields, allowing them to be represented as a sum of spherical harmonic terms. Spatial derivatives are approximated by finite differences. This algorithm's numerical efficiency derives from the diagonal representation of the scattering matrix. Boundary conditions are approximated by a method due to Marshak (1947). The resulting linear system of equation is solved iteratively by the conjugate-gradient method.

tinction and scattering functions embedded in two-dimensional space. Cloud distributions employed in this study are not truly representative of naturally occurring clouds. Instead, they have been kept sufficiently simple 1) to test the radiation model, 2) to help facilitate the interpretation of model results, and 3) so that all that can be learned from these simple models will also be applicable to more complex situations. This is not to detract from the generality of the radiative transfer model; more realistic cloud distributions can be accommodated, but at the expense of significant computing time.

The structure of this paper is as follows. Section 2 contains notes on the methodologies used in solving the two- or three-dimensional transport equation spanning the years from 1975 to 1992. This section also contains a description of the algorithms that were used to verify the correctness of the implementation of the Fourier–Riccati method. Section 3 gives some background to the Riccati formulation and develops the spectral model. In addition, connections to other methods are described and for the special case of a vertically uniform horizontally inhomogeneous cloud, a convolutional interpretation of the solution to the radiative transfer equation is offered. Section 4 establishes the connection between the particular Riccati formulation developed in this study to that employed in the solution to two-point boundary value problems. The section also discusses properties of the Fourier–Riccati equation such as its stability and efficiency, as well as technical matters concerning its numerical integration. In section 5, the implementation of the Fourier–Riccati method is tested by comparing numerical results to two other methods. The dependence of the radiance and flux on angular and spatial resolution are discussed while paying particular attention to comparisons of the independent pixel approximation.

2. Review of the literature

A perusal of the meteorological literature where radiative transfer theory is applied to clouds and atmospheres reveals that the majority of radiation calculations to date have been performed using plane-parallel models (e.g., Wiscombe 1983; Harshvardan 1991; Kattawar and Thompson 1991) whose input can only be a vertically stratified atmosphere. However, a growing awareness of the severe limitations imposed by

horizontally uniform media has prompted a number of investigators to develop radiative transfer models that can accommodate vertical and horizontal inhomogeneities of clouds. Since clouds are the prime source of variability of atmospheric radiation, there has been a sustained interest in treating even simple geometrical shapes such as cubes, spheres, cylinders, and paraboloids of revolution by various methods while maintaining internal uniformity (e.g., Busygin et al. 1973; McKee and Cox 1974; Davies 1976, 1978; Barkstrom and Arduini 1977; Cogley 1981; Welch and Zdunkowski 1981; Preisendorfer and Stephens 1984; Stephens and Preisendorfer 1984). Developments by Avaste and Vaynikko (1974), Busygin et al. (1977), Aida (1977), Glazov and Titov (1979), Titov (1979, 1980), Davies (1984), and others consisted in arranging these homogeneous clouds into periodic or uniformly random arrays in order to simulate cloud fields. By comparison, relatively little attention has been paid to systems with internal inhomogeneities. A broad review of such work on radiative transfer in nonuniform media carried out between 1955 and 1975 is given by Crosbie and Lindsenbardt (1978). Table 1 summarizes applications of radiative transfer theory to inhomogeneous media relevant to the atmospheric science community from 1975 to 1992. In almost all the examples cited in the table, the cloudy medium is assumed periodic with no horizontal boundary conditions imposed.

3. Spectral approach to radiative transfer

In order to address the issues presented in section 1, a general spectral formulation of the radiative transfer problem is developed for media embedded in three-dimensional space. Such a formulation is convenient as it provides a launch point for spectral approaches to one- and two-dimensional radiative transfer. In particular, it is conjectured that two-dimensional radiative transfer studies can address the aforementioned issues if the medium possesses arbitrary vertical and horizontal spatial variability. It is asserted that all of the numerical and interpretational difficulties associated with three-dimensional radiative transfer are encountered with radiative transfer in media embedded in two dimensions. This notion, pursued here, not only leads to economy in computation, but also lends itself easily to mathematical analysis and physical interpretation.

A prerequisite necessary for the development of the Fourier–Riccati radiative transfer model is the Fourier decomposition of the equation of transfer given in Stephens (1988). Only the final result for the three-dimensional RTE is given here:

$$\pm\mu_k \frac{\partial N_{uv}^{mc/s}(z, \mu_k)}{\partial z} = -\sum_{v'=-V}^{V}\sum_{u'=-U}^{U} \alpha(\delta u, \delta v; z) N_{u'v'}^{mc/s}(z, \pm\mu_k)$$

$$- \frac{i\pi\eta}{2(1+\delta_c\delta_m)} \sum_{m'=0}^{M} \{X_u^{c/s}(m, m') N_{uv}^{m'c/s}(z, \pm\mu_k) + Y_v^{c/s}(m, m') N_{uv}^{m's/c}(z, \pm\mu_k)\}$$

$$+ \frac{1+\delta_c\delta_m}{4} \sum_{v'=-V}^{V}\sum_{u'=-U}^{U} s(\delta u, \delta v; z) \{\sum_{j=1}^{N} w_j P^m(\mu_k, \mu_j) N_{u'v'}^{mc/s}(z, \pm\mu_j) + w_j P^m(-\mu_k, \mu_j) N_{u'v'}^{mc/s}(z, \mp\mu_j)\}$$

$$+ \frac{1+\delta_c\delta_m}{4} \sum_{v'=-V}^{V}\sum_{u'=-U}^{U} s(\delta u, \delta v; z) P^m(\pm\mu_k, \mu_0) N_{u'v'}^{0c/s}(z, -\mu_0) + Q_{u'}^m(z, \pm\mu_k), \quad (1)$$

where P^m is the mth Legendre component of the phase function expansion, $N_{u'}^0(z, \pm\mu_0)$ the Fourier component of the direct beam, $Q_{u'}^m(z, \pm\mu_k)$ an internal source function, and $\delta u = u - u'$, $\delta v = v - v'$. The quantities $X_u^{c/s}(m, m')$ and $Y_v^{c/s}(m, m')$ are related to the azimuthal coupling terms $D(m, m')$, $E(m, m')$, $F(m, m')$, and $G(m, m')$, obtained by integrating the RTE with respect to ϕ and defined in Stephens (1988). The designators c/s refer to the cosine and sine components of the radiance amplitudes, respectively, associated with the Fourier expansion of the total radiance. The modified coupling terms are defined as

$$X_u^c(m, m') = \frac{uD(m, m')}{2L_x},$$

$$Y_v^c(m, m') = \frac{vE(m, m')}{2L_y},$$

$$X_u^s(m, m') = \frac{uG(m, m')}{2L_x},$$

$$Y_v^s(m, m') = \frac{vF(m, m')}{2L_y}. \quad (2)$$

This linear system of ordinary differential equations given in (1) along with the Fourier transformed boundary conditions constitutes a two-point boundary value problem (BVP). One difference between the BVP developed here and that of Stephens (1986, 1988) is the explicit inclusion of the source terms. Whereas Stephens constrains the solar zenith angle to one of the quadrature angles, the solar zenith angle in this formulation is arbitrary, as it is also in Kobayashi (1991).

a. The Riccati transformation

The system of ordinary differential equations given by (1) is an example of a local formulation of radiative transfer, and has been solved for the radiances as a BVP via several techniques as shown in Table 1. By comparison, global formulations of interest here do not involve the radiances directly. Instead, the central concept is that of radiative responses of the optical medium to a distribution of source functions. These responses are defined by the reflection and transmission operators designated by **R** and **T**, respectively.

One reason for developing a response function formulation is that **R** and **T** are calculated from a numerically stable, parallel algorithm. In addition, the response functions are independent of the boundary conditions as will be demonstrated. This means that a change in the boundary conditions will not require a recalculation of these operators. Another reason for pursuing such an approach is that its rich physical and mathematical content allows for useful interpretations associated with the transfer process not easily accessible using other methods.

The radiative response operators can also be calculated by the doubling and adding method developed by Grant and Hunt (1969) and van de Hulst (1965). In those formulations, the composition relations for the reflection and transmission operators are developed for plane-parallel clouds of finite optical depth. Diner and Martonchik (1985) using the interaction principle developed adding and doubling relations to calculate three-dimensional radiative transfer in periodic inhomogeneous media bounded below by a surface with general reflection properties. Stephens (1986) in an independent work formulated a doubling relation used to determine radiances in vertically uniform media embedded in two-dimensional spaces.

If there is vertical variation in the extinction and scattering functions, then it becomes necessary to slice the cloud into slabs that are approximately internally vertically uniform, calculate the reflection and transmission functions via doubling for each slab, and then repeatedly use adding formulas to determine the global radiative responses of the entire cloud. In this kind of a situation, the optimal division of the medium into uniform layers is a trial and error process.

A differential formulation for **R** and **T** would circumvent this inconvenience (however, the issue of choosing the correct number of quadrature points, azimuthal modes, and spatial discretization will always exist), particularly when the cloudy medium is thick and exhibits rapid vertical spatial fluctuations. In this case an analysis of the equations could provide information relevant to step size selection. Better still, the differential equation solver could incorporate adaptive step size control (e.g., Press et al. 1988). Employing such a strategy is more efficient than trial and error since the number of layers and the thickness of each layer can be automatically computed. In practice, it has been observed that for vertically inhomogeneous, optically thick clouds embedded in two dimensions, combinations of doubling and adding can take significantly more time (twice as long in some cases) to compute than solving the differential equations for **R** and **T** when step size selection is deduced from stability considerations alone. Furthermore, the adding and doubling computation had to be performed several times to ascertain whether convergence in the solution had been attained. Even for plane-parallel geometry, adding and doubling for vertically inhomogeneous, thick media is computationally less efficient than other methods, such as the discrete ordinates method of Stamnes et al. (1988) (e.g., the well-known, heavily used DisORT radiation code).

Mathematical simplification is attained by transforming the partial differential equation of radiative transfer into an ordinary integro–differential equation depending only on the vertical depth z. Hence, the first step in realizing a response function formulation is the transformation of the horizontal gradients of the radiance to algebraic terms, accomplished in Eq. (1).

The transformation of (1) into an initial value problem (IVP) proceeds in two stages. First (1) is recast in matrix form as

$$\pm \frac{dN^{\pm}}{dz} = -\mathbf{t}N^{\pm} + \mathbf{r}N^{\mp} + Q^{\pm}, \tag{3}$$

where $N^{\pm}$ and $Q^{\pm}$ are the radiances and source functions in the positive (+) and negative (−) hemispheres (see also Fig. 1). Next, the interaction principle graphically illustrated in Fig. 1 is applied. The radiances and the global response operators can now be written as

$$\begin{aligned} N^{+}(z) &= R(z, b)N^{-}(z) + T(b, z)N^{+}(b) + \epsilon(b, z) \\ N^{-}(z) &= R(z, 0)N^{+}(z) + T(0, z)N^{-}(0) + \epsilon(0, z), \end{aligned} \tag{4}$$

where the term ϵ accounts for the internal or external sources. Inserting these relations into equations (3) yields

$$\frac{dR(z, b)}{dz} - R(z, b)\mathbf{r}R(z, b) + R(z, b)\mathbf{t} + \mathbf{t}R(z, b) - \mathbf{r} = 0$$

$$\frac{dT(b, z)}{dz} + R(z, b)\mathbf{r}T(b, z) + \mathbf{t}T(b, z) = 0$$

$$\frac{d\epsilon(b, z)}{dz} - R(z, b)\mathbf{r}\epsilon(b, z) - R(z, b)N_{-}^{0} + \mathbf{t}\epsilon(z, b) - N_{+}^{0} = 0$$

$$\frac{dR(z, 0)}{dz} + R(z, 0)\mathbf{r}R(z, 0) - R(z, 0)\mathbf{t} - \mathbf{t}R(z, 0) + \mathbf{r} = 0$$

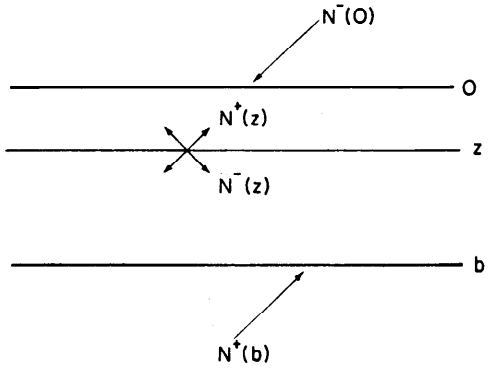

FIG. 1. Schematic representation of the interaction principle. A layer extending from $z = 0$ to $z = b$ is divided at z. The reflection operator is $R(z', b)$. Transmission operator $T(0, z')$. Pseudosource term $\epsilon(b, z)$. Suppressing the angular dependence, the radiance in the positive hemisphere at horizontal position coordinate s is

$$N^+(s, z) = R(s, s', z, b)N^-(s', z) + T(s, s', b, z)N^+(s', b) + \epsilon(b, z).$$

The radiance in the negative hemisphere is

$$N^-(s, z) = R(s, s', z, 0)N^+(s', z) + T(s, s', 0, z)N^-(s', 0) + \epsilon(0, z).$$

The reflection, transmission operators, as well as the pseudosource function are in general path dependent. The reflection and transmission operators contain two coordinates, s and s', in their argument because of the convolution between the extinction and radiance in the Fourier domain asserted by Eq. (1).

$$\frac{dT(0, z)}{dz} + R(z, 0)\mathbf{r}T(0, z) - \mathbf{t}T(0, z) = 0$$

$$\frac{d\epsilon(z, 0)}{dz} + R(z, 0)\mathbf{r}\epsilon(0, z) + R(z, b)N_+^0 - \mathbf{t}\epsilon(z, b) + N_-^0 = 0. \quad (5)$$

These six equations suffice to calculate the emerging radiances at the cloud boundaries or at any interior point within a cloud. The terms N_-^0 and N_+^0 are the radiances associated with single scattering in the lower and upper hemispheres. The first and fourth of the set of equations in (5) is known as the Riccati matrix differential equation (RMDE). Examples of IVPs, these equations have been studied in a more general form given by

$$\frac{dK(z, b)}{dz} - K(z, b)\mathbf{A}K(z, b) - K(z, b)\mathbf{B} - \mathbf{C}K(z, b) - \mathbf{D} = 0. \quad (6)$$

The RMDE plays a central role in many diverse fields such as control theory (Barnett 1984), neutron transport (Bellman 1970), and plasma physics. It also enters in the theory of Backlund transformations, used for solving for nonlinear partial differential equations. An analysis of its solutions using nonlinear superposition principles has been given by Harnad et al. (1983) and Rand and Winternitz (1984).

Returning to (5), the initial conditions required for its solution are

$$R(z = 0, 0) = 0 \quad R(z = b, b) = 0$$
$$T(z = 0, 0) = 1 \quad T(z = b, b) = 0$$
$$\epsilon(z = 0, 0) = 0 \quad \epsilon(z = b, b) = 0. \quad (7)$$

A cloud of zero optical thickness and a perfectly absorbing ground can have no diffusely reflected component, and any incident diffuse radiation is transmitted without attenuation or scattering. Hence, $R(0, z = 0) = 0$ and $T(0, z = 0) = 1$, respectively. The condition $\epsilon(0, z = 0) = 0$ states that in the absence of sources, there is no diffuse radiation. Six equations are required to specify the response functions of the medium because the integrals defining **R**, **T**, and ϵ are path dependent: integration from $z = 0$ to $z = b$ yields response functions differing from those obtained by integrating from $z = b$ to 0. If the internal radiances are also required, then (4) may be solved for $N^-(z)$ and $N^+(z)$. The results are

$$N^+(z) = (I - R(z, b)R(z, 0))^{-1} \times [T(b, z)N^+(b) + R(z, b)T(0, z)N^-(0) + R(z, b)\epsilon(0, z) + \epsilon(b, z)]$$

$$N^-(z) = (I - R(z, 0)R(z, b))^{-1} \times [T(0, z)N^-(0) + R(z, 0)T(b, z)N^+(b) + R(z, 0)\epsilon(b, z) + \epsilon(0, z)]. \quad (8)$$

According to Bellman (1970), Eqs. (5) are associated with the following picture: **r** can be identified with a single backscattering, **tR** corresponds to reflection followed by forward scattering, **Rt** corresponds to forward scattering followed by a reflection, and **RrR** corresponds to reflection, backscattering, and then reflection again.

These interpretations were originally applied to the RMDE describing particle propagation in a one-dimensional rod and extended to plane-parallel atmospheres described by Wing (1962). The scattering processes described above were formulated in physical space, whereas the RMDE of interest here is associated with two-dimensional radiative transfer formulated in the frequency domain. The response matrices are complex operators that depend on u, u', μ, μ', m, m', and z. They operate on the diffuse incident radiances [i.e., the Fourier transformed boundary conditions $N^-(0)$ and $N^+(b)$, which are functions of u', μ', and m'] resulting in radiances that depend on u, μ, and m. Because the operators **R** and **T** are generally full matrices, the spatial (and angular) coupling of the radiance to the cloudy medium can be long range and strong.

This contrasts with plane-parallel atmospheres where there is no horizontal scale dependence: the extinction and scattering functions are constants. Fourier trans-

forms of these functions are delta distributions. Hence, the convolution required by (1) decouples in u, and in azimuth m, since there is contribution only by the domain average component $u = 0$. This result has bearing on the independent pixel approximation, since the local application of plane-parallel calculations negates the possibility of scale coupling.

b. Radiative transfer in the frequency domain: Connection with other methods

By reformulating the equation of transfer as a boundary value problem in one dimension, all the formalism and computational techniques that describe scattering in plane-parallel media carry over to the horizontally inhomogeneous case. In addition, the developments here are intimately tied to issues concerning existence and stability of the RMDE, pursued in the Appendix. Finally, the results presented here associate scattering as a filtering operation in the frequency domain and lead to a computational technique for determining the radiance field at any point within the cloudy medium (Flatau and Stephens 1990).

Beginning with Eqs. (3), two new sets of radiances are defined:

$$\tilde{\aleph}(z) = \begin{bmatrix} N^+(z) \\ N^-(z) \end{bmatrix} \quad \tilde{\aleph}_\epsilon = \begin{bmatrix} N_\epsilon^+(z) \\ N_\epsilon^-(z) \end{bmatrix}, \tag{9}$$

where $\tilde{\aleph}(z)$ is a vector of radiances emerging at vertical position z inside the medium, and $\tilde{\aleph}_\epsilon(z)$ is the single-scattering source vector. By defining the system matrix $\mathbf{A}(z)$ as

$$\mathbf{A}(z) = \begin{pmatrix} -\mathbf{t}(z) & \mathbf{r}(z) \\ -\mathbf{r}(z) & \mathbf{t}(z) \end{pmatrix}, \tag{10}$$

Eq. (3) can be written as

$$\frac{d\tilde{\aleph}(z)}{dz} = \mathbf{A}(z)\tilde{\aleph}(z) + \tilde{\aleph}_\epsilon(z). \tag{11}$$

The homogeneous solution to this equation,

$$\frac{\phi(z)}{dz} = \mathbf{A}(z)\phi(z), \tag{12}$$

can be explicitly represented in component form as

$$\phi(z) = \begin{pmatrix} \phi_{11}(z, 0) & \phi_{12}(z, b) \\ \phi_{21}(z, 0) & \phi_{22}(z, b) \end{pmatrix}, \tag{13}$$

and the complete solution to this problem can be formally written as

$$\begin{bmatrix} N^+(z) \\ N^-(z) \end{bmatrix} = \phi(z)\Big\{(\mathbf{M}_u\phi(b) + \mathbf{M}_d\phi(0))^{-1} \times \Big[B - \mathbf{M}_u\phi(b)\int_0^b \phi(t)^{-1}\tilde{\aleph}_\epsilon(t)dt\Big]\Big\} + \phi(z)\int_0^z \phi(t)^{-1}\tilde{\aleph}_\epsilon(t)dt, \tag{14}$$

where

$$B = \begin{pmatrix} N^+(z = b) \\ N^-(z = 0) \end{pmatrix},$$

$$\mathbf{M}_u = \begin{pmatrix} \mathbf{1} & \mathbf{0} \\ \mathbf{0} & \mathbf{0} \end{pmatrix}, \quad \text{and} \quad \mathbf{M}_d = \begin{pmatrix} \mathbf{0} & \mathbf{0} \\ \mathbf{0} & \mathbf{1} \end{pmatrix}.$$

In the case of a vertically uniform, horizontally inhomogeneous cloud, the solution of (12), known as the propagator, is $\phi(z) = \exp(\mathbf{A}z)$. If the cloudy medium is vertically nonuniform, then it can be sliced into thin slabs such that within each slab the propagator is constant. Then, the propagator for the entire medium can be written as a product of individual propagators (Gantmacher 1959; Gilbert and Backus 1966; Karp et al. 1980) corresponding to each of the slabs, paying attention to vertical ordering of the slabs since the propagators in general will not commute:

$$\phi(z) = \phi(z, z_{k-1})\phi(z_{k-1}, z_{k-2}) \times \cdots \times \phi(z_1, 0). \tag{15}$$

Since the boundary conditions are specified, it is possible to use (14) and (15) to determine the radiation at all k levels. All of the aforementioned calculations are performed in the frequency domain, and the radiances in the spatial domain are recovered by taking the inverse Fourier transform of $\tilde{\aleph}(z)$.

The notion that multiple scattering acts to smooth the radiation field even though the cloud field can be extremely inhomogeneous can now be addressed. From a purely mathematical point of view, the radiance vector must generally be smoother than $\mathbf{A}$ or $\tilde{\aleph}_\epsilon$ because if these functions have m derivatives, $\tilde{\aleph}(z)$ must have $m + 1$ derivatives as seen from (11). More physically, the propagator contains information about the optical properties of the medium (assumed here to be vertically uniform) as well as azimuthal and angular information.

The propagator does not of itself constitute a solution to the radiative transfer equation unless boundary conditions are imposed. Furthermore, because the propagator depends on the *difference* between spatial coordinates [e.g., Eq. (14)], it has the effect of weighting the single scattering source function by the same amount everywhere inside the medium. This convolution diminishes the magnitudes of all high-frequency components in $\tilde{\aleph}_\epsilon(z)$. In physical space this corresponds to a smoothing of the radiances by the small-scale structures of the cloud field.

4. Solution procedures

The formulation of a Fourier–Riccati approach to solving the equation of transfer has proceeded in two steps: transformation of the general equation of transfer into a one-dimensional two-point BVP in Fourier space, followed by subsequent transformation to an IVP via the interaction principle. The first step was

performed because linear ordinary differential equations are more amenable to analyses than partial differential equations. The second step develops the Riccati method, which dissociates the radiation field from the optical properties of the medium. The emerging radiation field is the response of global transmission and reflection operators to prescribed boundary conditions. These operators are independent of the boundary conditions and can be calculated by numerical procedures commonly used in plane-parallel theory.

The structure of the local reflection and transmission operators (matrices) associated with media embedded in two- and three-dimensional spaces differ substantially from their plane-parallel counterpart due to the presence of the horizontal gradient terms. In addition, plane-parallel theory, generally formulated in physical space, is not encumbered with complex quantities. Although techniques for solving plane-parallel atmospheres are applicable here, their use is not necessarily optimum from a numerical standpoint for the inhomogeneous case. The numerical solution of (5) as well as the efficiency of the algorithm used to obtain numerical results will now be discussed. Details concerning the uniqueness and stability of the Fourier–Riccati method are addressed in the Appendix.

a. Numerical considerations

The system of nonlinear matrix differential equations (5) has been successfully integrated using a fourth-order Runge–Kutta solver with a high degree of accuracy as will be seen in two dimensions. The accuracy of the radiance and flux fields depends crucially on a number of factors: spatial sampling of the extinction and scattering functions, vertical step size selection, and quadrature scheme. Prior to performing any calculations, the spatial sampling frequency of the medium's optical properties is determined by visually inspecting a surface plot of $\alpha(u, z)$ and $s(u, z)$, the Fourier transforms of the extinction and scattering functions, respectively. The sampling rate is selected for the function having the highest cutoff frequency [the frequency at $\alpha(u, z)$ or $s(u, z)$ are zero] at some value $z = z'$. This is to some extent a trial-and-error process and depends on the fidelity desired of the inverse Fourier transform to reproduce the original function. The calculation of the Nyquist or sampling frequency that must be used to avoid aliasing follows: the function is sampled at twice the highest frequency present in the Fourier spectrum. It may happen that the spectrum is not band limited in the sense of there not being some highest cutoff frequency at which the transform of the function goes to zero. In that case it is necessary to band limit the function by appropriately filtering it and redoing the spectral analyses. This will introduce some bias in the radiation field, since the smallest scale structures present in the cloud are either removed or greatly attenuated. This bias may or may not be important depending on the intended application.

One way of exploring the spatial sampling issue is by simulating a cloudy medium possessing different scales of variability. For purposes of this discussion, the vertically uniform extinction function:

$$\alpha(x) = 1 + \frac{1}{4}\sin\left(\frac{\pi x}{2}\right) + \frac{1}{2}\sin\left(\frac{7\pi x}{2}\right) \quad (16)$$

is considered (Fig. 2). The mean optical depth of such an extinction is unity and the phase function has been set to be isotropic. The smallest scale structure can be resolved by sampling this function at twice the highest spatial frequency according to the Nyquist theorem. The highest frequency is 1.75 km^{-1}. Therefore, the spatial sampling rate must be 3.5 km^{-1} or 285.7 m. This function was chosen since its energy density at the highest frequency (1.75 km^{-1}) is greater than that at (0.25 km^{-1}) by a factor of 4.

It should be noted that such an extinction function can never be representative of any naturally occurring cloud since it states that there is more cloudy matter in shorter as opposed to longer space scales. While this function is at variance with spectral analyses of cloud liquid water content that suggest that clouds are scale invariant over a large range of spatial scales, it dramatically highlights the effects of incorrect sampling rate, which is the intended purpose of this simple example.

Two numerical experiments were performed. The first fixed the sampling rate at 250 m, the second at 500 m. Sampling at 500-m resolution aliases the highest frequency component of $\alpha(x)$. The results of these experiments, presented in Figs. 3a–d, point to a sensitivity of the radiances due to inadequate sampling that is not shared to the same extent by the fluxes. The largest

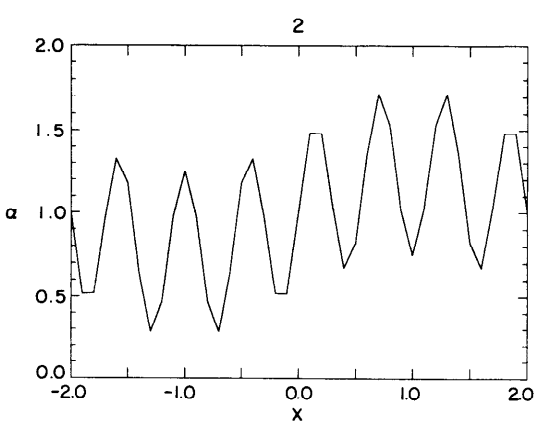

FIG. 2. Spatial variation of the extinction density used to investigate the effects of spatial sampling. The function plotted is

$$\alpha(x) = 1 + \frac{1}{4}\sin\left(\frac{\pi x}{2}\right) + \frac{1}{2}\sin\left(\frac{7\pi x}{2}\right).$$

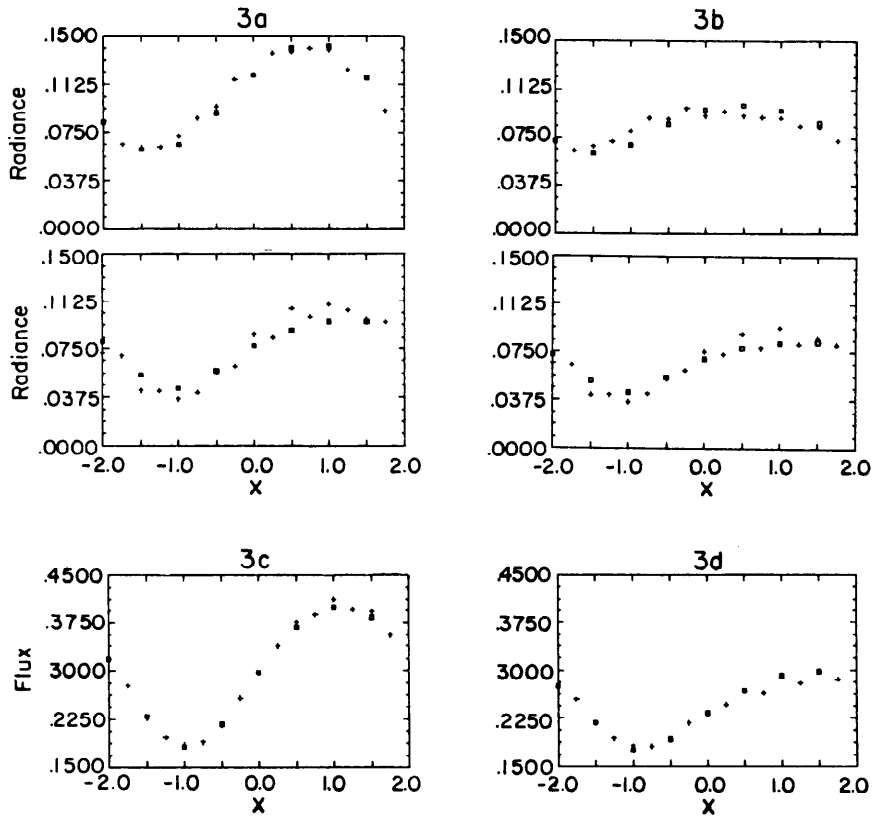

FIG. 3. (a) Upwelling radiances exiting the upper surface of a cloud whose extinction density is plotted in Fig. 2. The cloud was sampled at two different spatial resolutions, 250 m (clear cells) and 500 m (crosses). Radiances top to bottom are calculated for an observation angle of 58.7° and 16.2°. The solar zenith angle is 30°. Scattering is conservative with an isotropic phase function. Calculations were performed using 8 streams and 8 azimuthal components. (b) As in (a) but for downwelling radiances at the lower cloud boundary. (c) Upwelling fluxes exiting the upper surface of a cloud whose extinction density is plotted in Fig. 2. The cloud was sampled at two different spatial resolutions 250 m (clear cells) and 500 m (crosses). The solar zenith angle is 30°. Scattering is conservative with an isotropic phase function. (d) As in (c) but for downwelling fluxes at the lower cloud boundary.

differences between the reflected radiances sampled at the aforementioned resolutions is about 18% (lower plot in Fig. 3a). For the transmitted radiances it is 11% (lower plot in Fig. 3b). The observing angle is 16.2°; the incident solar irradiance is 30°. Both angles are measured with respect to a vertical in the first quadrant. In the worst case, fluxes differ by about 5%. This is expected since flux, being the first angular moment of the radiance, is smoother than the radiance.

b. Treatment of the direct beam and efficiency considerations

Once the spatial sampling frequency is calculated, the circulant matrices $\alpha(u, u', z)$ and $s(u, u', z)$ are easily created. It is at this point where spectral methods in general become numerically inefficient by comparison to direct approaches. The reason is that simple scalar multiplication of two functions in the spatial domain is replaced by the much more complex convolution operation in the frequency domain.

Convolution, however, can be efficiently performed. Consider for example the external source term in the frequency domain:

$$\frac{1 + \delta_c \delta_m}{4} \sum_{v'=-V}^{v'=V} \sum_{u'=-U}^{u'=U} s(\delta u; z) \times P^m(\pm\mu_k, \mu_0) N^{c/s}_{u'v'}(z, -\mu_0). \quad (17)$$

This convolution between the direct beam along a trajectory specified by μ_0 with the scattering function s can be efficiently and easily evaluated by taking the Fourier transform of the product: $[\alpha(x, z)N(z, -\mu_0)]$. This method was also used by Kobayashi (1991).

The criterion used to determine the vertical step size for the integration of (5) is based on a simple scale analysis of the **A** matrix [Equation (10)], that is, num-

ber of steps = $\max\|\mathbf{A}\|$ over the interval $0 \leq z \leq b$. The step size is determined by taking the inverse of the number of steps. While in practice this selection has always worked, in many cases it was possible to carry out the integration using large steps without encountering a numerical explosion or significant loss of accuracy. Therefore, this criterion of step selection is too conservative. A solution here would be to incorporate a variable step size algorithm in the Runge–Kutta solver. The undesirable feature of a variable step algorithm is primarily associated with the interpolation procedure that would have to be employed in order for the internal radiance fields to be evaluated at some prescribed position inside the medium after the **R** and **T** matrices have been calculated. Such an interpolation may compromise the accuracy of the solution. Since the radiances in this paper are calculated only at the cloud boundaries, a variable step algorithm may increase the efficiency of the Runge–Kutta IVP solver, but that option was not explored.

To allow for the possibility of taking larger steps, a single-Gauss instead of a double-Gauss quadrature scheme was used. The former always yields a larger minimum value of μ_k over an angular interval than the latter, and the number of steps is inversely proportional to μ_k. This inverse relationship can cause the RMDE to become stiff and potentially expensive to solve. The expense is associated with the number of complex floating point operations per step. Most of the calculational cost is consumed by the RMDE, requiring four complex matrix multiplications per step. To minimize this cost, a combination of different strategies was employed. First, it is noted that the calculation of the global transmission operator is not required if the radiation fields are to be calculated at the boundaries of the cloudy medium. Next, the sparsity of the **r** and **t** matrices is exploited in connection with the observation that the Riccati equations can be factored. For example,

$$\frac{d\mathbf{R}(z,0)}{dz} = (-\mathbf{t} + \mathbf{R}(z,0)\mathbf{r})\mathbf{R}(z,0) - \mathbf{R}(z,0)\mathbf{t} + \mathbf{r} = 0. \quad (18)$$

The matrix multiplication $\mathbf{R}(z,0)\mathbf{r}$ is that of a full matrix by a sparse matrix as is $\mathbf{R}(z,0)\mathbf{t}$.

The term $(-\mathbf{t} + \mathbf{R}(z,0)\mathbf{r})\mathbf{R}(z,0)$ is the product of two full matrices. Two effective ways of calculating the product are by exploiting the parallelism in matrix multiplication on a parallel computing machine (such as the Cray YMP) or algorithmically, using fast matrix multiply routines such as Winograd's variation of Strassen's algorithm. The latter is implemented in the BLAS library under the subroutine CGEMMS and falls in the class of "asymptotically fast algorithms." This means that gain in speed is attained only for very large matrices. The complexity of the algorithm varies as $N^{2.8}$ instead of N^3 associated with conventional multiplication. Using this algorithm for the size of matrices in this study where N varied between 512 and 1024 elements, yielded a speed increase of nearly a factor of four over the brute-force approach. This timing is similar to that using conventional matrix multiplication where the parallelization option of the compiler is engaged. For larger matrices, the algorithmic approach will prevail

5. Discussion of numerical results

In this section the implementation of the Fourier–Riccati model is tested by comparing numerical results to Monte Carlo simulations (O'Brien 1991) and the spherical harmonic spatial grid (SHSG) method of Evans (1992) for several combinations of solar geometry and optical properties of the medium. Beyond model verification, this section begins to explore the issue of how accurately radiances and fluxes may be calculated, given prescribed spatial discretization of the medium and prescribed angular resolution of the phase function. In view of the great usage of plane-parallel calculations, in particular of the so-called independent pixel approximation, numerical comparisons of radiances and fluxes between the one- and two-dimensional radiative transfer models is also included and discussed.

In order to establish the correct working of the Fourier–Riccati model, the following cases were examined: isotropic conservative and nonconservative scattering with Gaussian extinction and scattering functions, conservative and nonconservative scattering with asymmetric Henyey–Greenstien phase functions, and asymmetrical raised sine function defining the extinction and scattering. In all cases the medium was illuminated obliquely at a solar zenith angle of 30° and the vertical variation of the medium was linear. The choice of extinction and scattering functions was dictated by spatial symmetry/asymmetry considerations. Unlike the implementation of Stephens (1986) that could accommodate only even extinction and scattering functions, this formulation allows for combinations of either.

a. Radiance and flux distributions

Figures 4a and 4b offer comparisons of the emerging radiances calculated at the boundaries of a cloudy atmosphere using the Fourier–Riccati model to those obtained via Monte Carlo and SHSG using an eight-stream approximation of the phase function and eight azimuthal modes. Figures 4c and 4d show corresponding flux comparisons. It is observed that the upwelling radiances are more accurately calculated than the downwelling radiances at low observation angles. As the viewing angle approaches nadir, the radiances are computed much more accurately. Fluxes by comparison are in relatively good agreement with the other methods. This is because integration of the radiances

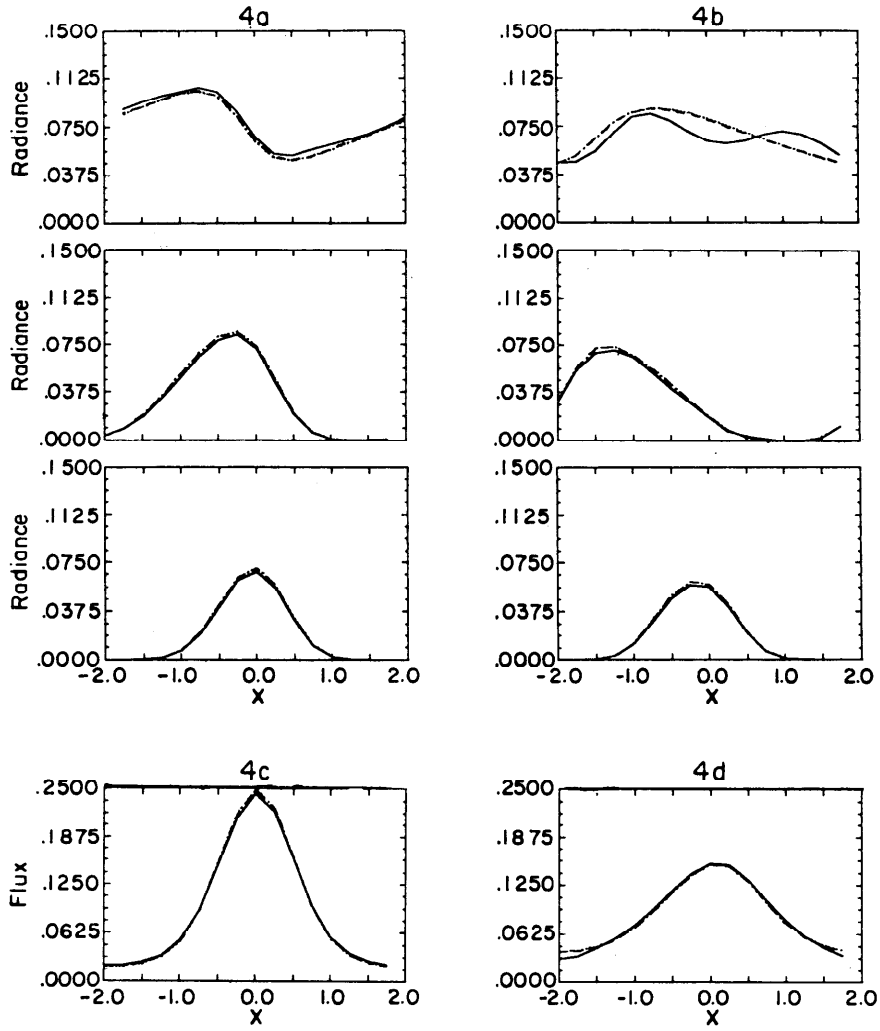

FIG. 4. (a) Comparison of upwelling radiances calculated by the Fourier–Riccati model (solid line corresponds to 8 streams and 8 azimuthal components) to those calculated by the spherical harmonic spatial grid method (dotted line) (Evans 1992) and accelerated Monte Carlo method (fine dashed line) (O'Brien 1992). Cloud extinction density is given by $\alpha(x, z) = 2(1 - z \times \exp(-\pi x^2)$. Scattering is conservative with an isotropic phase function. The solar zenith angle is 30°. Top to bottom, the observation angles are 79.6°, 58.7°, and 16.2°. Radiances are calculated at upper cloud boundary. (b) As in (a) but for downwelling radiances at the lower cloud boundary. (c) Comparison of upwelling fluxes calculated by the Fourier–Riccati model (solid line corresponds to 8 streams and 8 azimuthal components) to those calculated by the spherical harmonic spatial grid method (dotted line) (Evans 1992) and accelerated Monte Carlo method (fine dashed line) (O'Brien 1992). Cloud optical properties and illumination geometry as in (a). Radiances are calculated at upper cloud boundary. (d) As in (c) but for downwelling fluxes at the lower cloud boundary.

to obtain fluxes damps oscillations of the former, resulting in a smooth flux field. Deviations in the fluxes are ascribed to inaccuracies of the radiances at low angles of observation.

The poorer agreement of the downwelling radiances can be physically explained in terms of the number of scatterings a photon experiences before exiting the medium. This number is dependent on the phase function, optical density of the medium, and its geometry. Qualitative reasoning suggests that for the isotropic phase function and extinction function of this example, most of the photons will be scattered backwards in the first couple of scattering paths near the top boundary of the Gaussian cloud where the extinction density achieves its maximum. This cloud is tenuous even at the origin where the (vertical) optical depth is unity; hence, low-order scattering prevails. However, those photons exiting the base of the cloud at low observation angles have had to been scattered several times because the optical pathlength can become large. In that case as in

plane-parallel theory, more quadrature points and azimuthal angles would be required to represent these radiances. To test this idea, the model was run again, this time with an "inverted" optical density function that had a minimum at the top boundary of the cloud. The extinction function used was $(z)\exp(-\pi x^2)$ instead of $(1 - z)\exp(-\pi x^2)$. In accordance with expectations, the downwelling radiances and fluxes were more accurately calculated than those emerging at the upper boundary.

A more demanding test of the Fourier–Riccati model is its requirement of accommodating nonsymmetric optical properties and nonisotropic phase functions. A harmonically varying cloud

$$\alpha(x, z) = 2(1 - z)(1 + \sin(0.5\pi x),$$

$$s(x, z) = \alpha(x, z)$$

and a Henyey–Greenstien phase function with $g = 0.5$ was introduced to determine the model's performance. Figures 5a and 5b compare the radiances exiting the

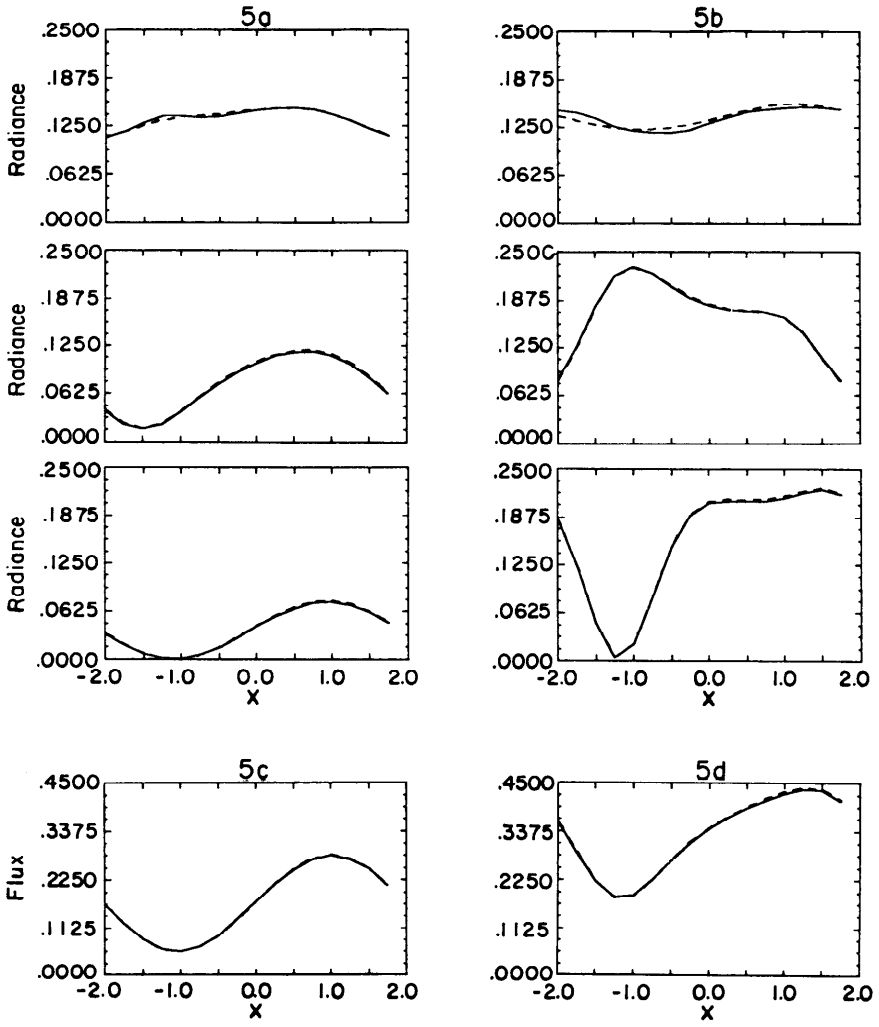

FIG. 5. (a) Comparison of upwelling radiances calculated by the Fourier–Riccati model (solid line corresponds to 8 streams and 8 azimuthal components) to those calculated by the spherical harmonic spatial grid method (dotted line) (Evans 1992) and accelerated Monte Carlo method (fine dashed lined) (O'Brien 1992). Cloud extinction density is given by $\alpha(x, z) = 2(1 - z)(1 + \sin(.5\pi x))$. Scattering is conservative $(s(x, z) = \alpha(x, z))$ with Henyey–Greenstein phase function $(g = .5)$. The solar zenith angle is 30°. Top to bottom, the observation angles are 79.6°, 58.7°, and 16.2°. Radiances are calculated at upper cloud boundary. (b) As in (a) but for downwelling radiances at the lower cloud boundary. (c) Comparison of upwelling fluxes calculated by the Fourier–Riccati model (solid line corresponds to 8 streams and 8 azimuthal components) to those calculated by the spherical harmonic spatial grid method (dotted line) (Evans 1992) and accelerated Monte Carlo method (fine dashed line) (O'Brien 1992). Fluxes are calculated at upper cloud boundary. Cloud optical properties and illumination geometry as in (a). (d) As in (c) but for downwelling fluxes at the lower cloud boundary.

boundaries of this cloudy medium calculated by the Fourier–Riccati and the SHSG methods. Figures 5c and 5d illustrate the corresponding flux comparisons. Excluding the lowest angle of observation (79.4°), radiances differ by 3%, fluxes within 0.5% (worst case figures).

One observation concerning the flux is the high angular resolution that is required to represent it. Unlike plane-parallel theory where two streams can yield flux calculations to high accuracy, scattering in an inhomogeneous medium seems to preclude such a simplification. To see this, consider Figs. 6a and 6b. Deviations of the fluxes from either the Monte Carlo or SHSG benchmarks are attributed to inaccuracies in the radiances. Since the flux is derived from the first angular moment of the radiance field, large deviations in the latter will result in errors in the fluxes. The large discrepancies observed, first thought to be a programming fault, are actually a phenomenon induced by weak spatio-angular coupling of the radiance to the cloudy medium by the $X_u^c(m, m')$ terms.

To understand what is meant by such a coupling, consider the case of scattering by an isotropic phase function in a plane-parallel layer. Only the $m = 0$ component suffices to calculate either the radiances or fluxes. Radiances are accurately calculated by using more streams, but again only the $m = 0$ azimuthal component contributes. This contrasts with two-dimensional radiative transfer where the quadrature angles and spatial components mix in the X_u^c matrix (in the plane-parallel mode of the Fourier–Riccati model, only the $u = 0$ component is sufficient to calculate radiances; therefore the X_u^c matrix is zero). It is this mixing that gives rise to an azimuthally asymmetrical radiance distribution. Hence, even though all the phase matrix elements associated with $m > 0$ are equal to zero, a large number of azimuthal modes may be required because that particular mode is coupled to higher-order modes. This may require a large number of angular quadrature components to ensure appropriate representation or sampling of the radiances prior to their integration to obtain fluxes.

The number of possible azimuthal modes is related to the number of quadrature angles via the addition theorem for spherical harmonics. Also noted is the fact that while the total flux exiting the cloud boundaries conserves energy to high accuracy, the spatial flux distributions can be in gross error. This is because energy conservation, the result of phase function normalization (and conservative scattering), is by itself insufficient to ensure convergence.

b. The independent pixel approximation

Two features evident from an examination of Figs. 4a and 4b are the asymmetry of the radiances and fluxes even when the medium is spatially symmetric and the position of the maximum radiance in relation to the position of the maximum extinction density. These features are unique to radiative transfer performed in two or three dimensions and are not reproducible by plane-parallel calculations. This is confirmed by Figs. 7a–d and 8a–d, which compare the radiances and fluxes exiting the cloud boundaries calculated by the independent pixel approximation and the Fourier–Riccati model. It is seen that the plane-parallel radiances and fluxes compare poorly. Radiances computed by the independent pixel approximation have the wrong shape and are, in the case of the Gaussian cloud, symmetric. Fluxes are also in disagreement with those calculated by the Fourier–Riccati method. These large differences are the result of light exiting from the sides of the clouds and have no equivalent in plane-parallel theory. As an aid to visualizing the relationship of the radiance fields to the optical properties of the medium, Figs. 9a and 9b are presented. Figure 9a relates the radiance field to a Gaussian extinction function, whereas Fig. 9b re-

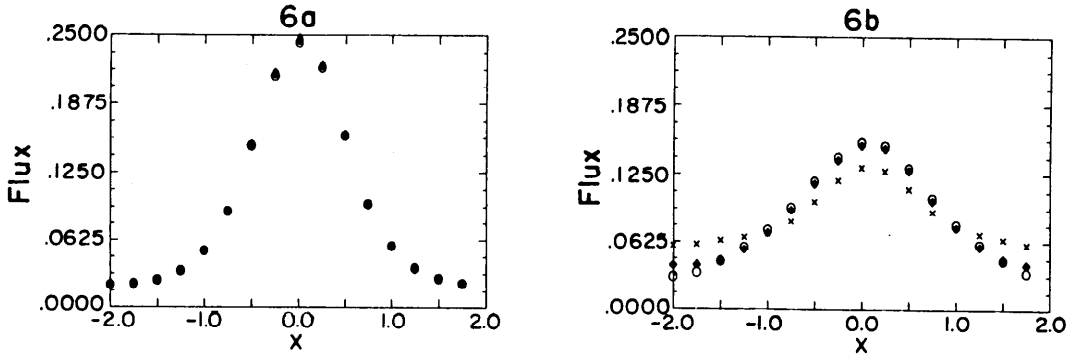

FIG. 6. (a) Comparison of upwelling fluxes calculated by the Fourier–Riccati model (solid diamonds corresponds to 10 streams and 10 azimuthal components, clear circles correspond to 8 streams and 8 azimuthal modes, crosses correspond to 4 streams and 4 azimuthal modes) to those calculated by the Spherical Harmonic Spatial Grid method (clear diamonds—not visible in the figure) (Evans 1992) and accelerated Monte Carlo method (dots—not visible in the figure) (O'Brien 1992). Cloud optical properties and illumination geometry as in Fig. 4a. Panel (b) As in (a) but for downwelling fluxes at lower cloud boundary.

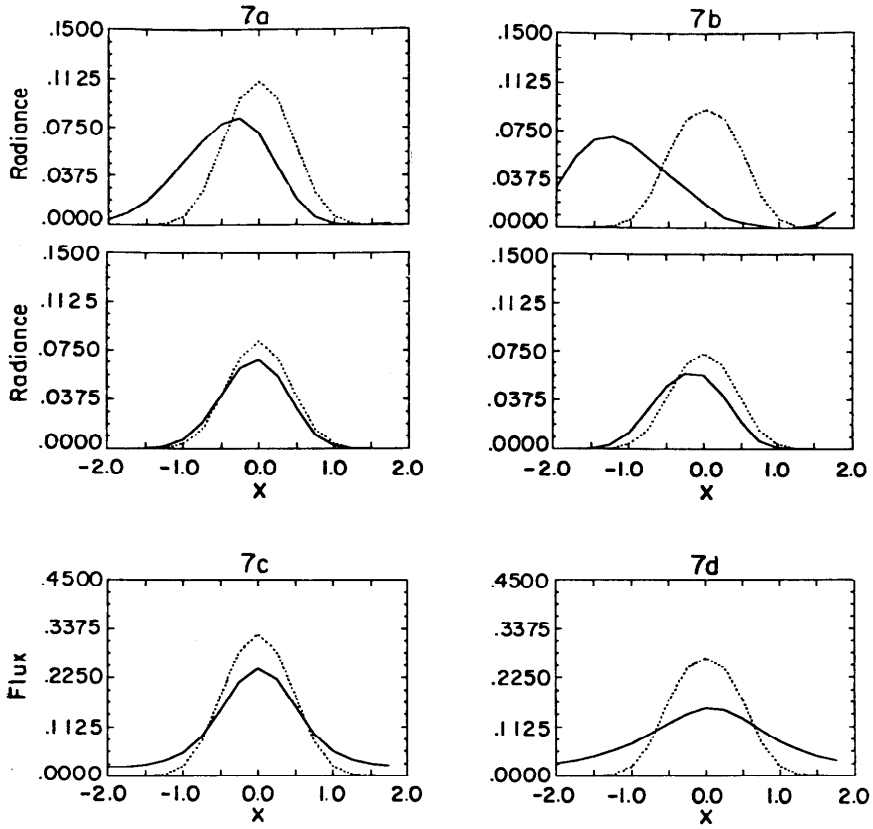

FIG. 7. (a) Comparison of upwelling radiances calculated by the Fourier–Riccati model (solid line corresponds to 8 streams and 8 azimuthal components) to those calculated by the independent pixel approximation (dots). Cloud optical properties and illumination angle are as in Fig. 4a. Top to bottom, the observation angles are 58.7° and 16.2°. Radiances are calculated at upper cloud boundary. (b) As in (a) but for downwelling radiances at lower cloud boundary. (c) Comparison of upwelling fluxes calculated by the Fourier–Riccati model (solid line corresponds to 8 streams and 8 azimuthal components) to those calculated by the independent pixel approximation (dots). Cloud optical properties and illumination angle are as in Fig. 4a. (d) As in (c) but for downwelling radiances at lower cloud boundary.

lates the radiance field to a harmonically varying extinction. In these figures gray levels represent densities of the extinction function. The magnitudes and directions of the radiances are represented by the lengths and angles of the lines drawn at the cloud boundaries.

c. Spatially averaged properties

A common practice in remote sensing applications is to approximate the domain averaged radiances by a plane-parallel layer having a mean optical thickness equal to that of an inhomogeneous cloud in situ. The attempt here is to gain information about the optical properties of the cloud (e.g., its phase function) by examining the angular distribution of the reflected radiances. To test this idea, the domain-averaged reflected radiances have been compared to those calculated by a plane-parallel model at the same observation angles. The results of these comparisons are presented in Figs. 10a and 10b. It is seen that differences in the worst case (at 58.7°) are about 25%, while at other angles the agreement is better. Caution should be exercised when interpreting these results, however. In practice, the differences may be much larger because natural clouds possess much greater variability than those studied here.

6. Conclusions

A method for solving the RTE for inhomogeneous media embedded in two and three dimensions has been developed based on the idea of eliminating the horizontal radiation advection terms by Fourier decomposition of the radiance fields. The resulting one-dimensional ordinary differential equation, a two-point BVP, is converted to an IVP by the principle of interaction. This procedure leads to a complex nonlinear system that defines the global reflection and transmission operators. These operators are independent of the boundary conditions and directly show the importance

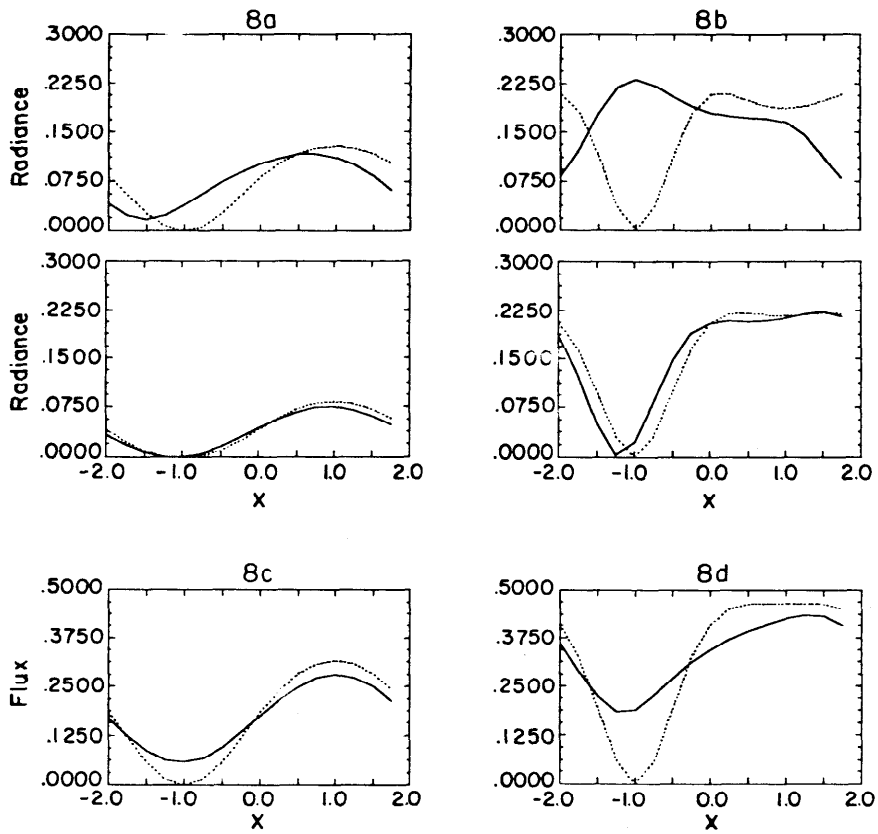

FIG. 8. (a) Comparison of upwelling radiances calculated by the Fourier–Riccati model (solid line corresponds to 8 streams and 8 azimuthal components) to those calculated by the independent pixel approximation (dots). Cloud optical properties and illumination angle are as in Fig. 5a. Top to bottom, the observation angles are 58.7° and 16.2°. Radiances are calculated at upper cloud boundary. (b) As in (a) but for downwelling radiances at lower cloud boundary. This figure as well as Figs. 7a and 7b show that the independent pixel approximation yields better agreement in the radiances as compared to those calculated by the Fourier–Riccati method (or, for that matter, the SHSG or accelerated Monte Carlo methods) provided that the emerging radiances are observed at nadir or at zenith. This suggests that if the vertically integrated optical thickness of a cloud and the solar zenith angle are known, measurements of the radiance at the external cloud boundaries taken at nadir or zenith will best agree with radiances calculated by plane parallel theory. However, the fluxes can still be in great error, as the figures illustrate. (c) Comparison of upwelling fluxes calculated by the Fourier–Riccati model (solid line corresponds to 8 streams and 8 azimuthal components) to those calculated by the independent pixel approximation (dots). Cloud optical properties and illumination angle are as in Fig. 5a. Radiances are calculated at upper cloud boundary. (d) As in (c) but for downwelling radiances at lower cloud boundary.

of scale dependence of the radiance fields. The method was implemented in order to explore several issues: how the accuracy of the calculated radiance and flux fields is affected by angular and spatial resolution and the extent of validity of employing the individual pixel approximation.

The implementation was tested by comparing numerical results with Monte Carlo and spherical harmonic spatial grid methods for various combinations of solar geometry and optical properties of the cloudy medium. In all cases the flux distributions exiting the cloud boundaries were in excellent agreement. Radiance distributions also agreed well, except those associated with the lowest angle of observation.

Although the models used to simulate the extinction, scattering, and phase functions are unrealistic (serving only to assist in the interpretation of the diffuse radiation fields they create), some useful and interesting results were obtained that may remain applicable in calculations involving much more inhomogeneous cloud structures and more realistic phase functions. For the cloudy media studied in this paper, the main conclusions are as follows.

1) The spatial flux distribution required a relatively large number of quadrature and azimuthal points (8 or more) for its accurate calculation using an isotropic phase function. Just as many quadrature and azimuthal

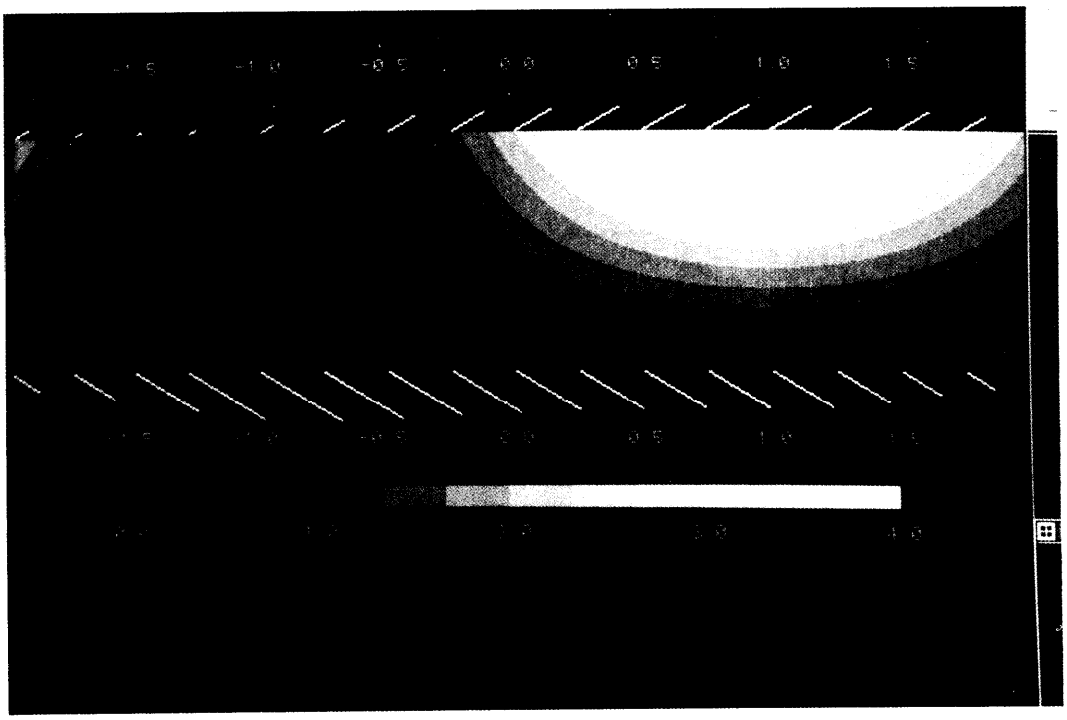

FIG. 9a. This image relates cloud extinction density to the cloud radiances exiting at the cloud boundaries. The length and direction of the processes emerging from the cloud are intended to illustrate the relative magnitudes of the radiances. The source (not shown) is located on the top right-hand side of the image, inclined 30° relative to a vertical axis. The extinction function and optical properties of the medium are as specified in Fig. 4a. The image shows that the greatest magnitude of the radiance does not occur at the point where the vertical optical thickness is greatest (in this case $\tau_{max} = 1.0$ at the origin), as would be predicted by the independent pixel approximation. Furthermore, the radiances are asymmetrically distributed. The independent pixel approximation would produce a symmetrical radiance and flux distribution.

points were required to calculate the spatial radiance distributions accurately. This result is not an artifact of the Fourier–Riccati model; the same effect was also observed using the spherical harmonic spatial grid method of Evans (1992) using the same media and imposing identical boundary conditions. The extent of validity of these observations is presently unknown. If generally true, they would preclude the possibility of calculating fluxes by approximating the RTE as a two-stream model as can be done for plane-parallel clouds.

2) The problem with a highly forward-peaked phase function, as is well known, is the large number of azimuthal components necessary for its spherical harmonic representation. This problem persists in radiation calculations performed in media embedded in two- or three-dimensional space. Radiative transfer in two or three dimensions is more complex than in plane-parallel atmospheres because horizontal derivatives of the radiances tightly couple spatial and angular information in the transfer equations. This coupling can yield an erroneous spatial flux distribution even though energy is conserved over the spatial domain of the cloud. If the spatial sampling of the cloud is correct, then increasing the (Gaussian) quadrature points, the number of azimuth modes, or both can substantially reduce the error. For a strongly forward-peaked phase function, a large number of quadrature angles and azimuthal modes would be required, resulting in extremely long computation times.

3) The effects of spatial sampling of optical properties of clouds appear to affect radiance calculations more adversely than fluxes. For the example studied in section 4, radiances calculated for aliased clouds differed from their correctly sampled counterparts by as much as 18%, whereas fluxes differed by only 5%. The sampling issue is relevant to remote sensing applications where inferences regarding cloud optical properties such as optical thickness or even phase functions are required. In such situations errors in the radiance fields may introduce large errors in the sought quantities in view of the nonlinear relation between the cloud and its radiative response.

4) The independent pixel approximation has not been found to be accurate using the clouds modeled in this paper. Spatial radiance and flux distributions in the visible and near-infrared portion of the solar spectrum calculated by this approximation differ in shape and in magnitude from those calculated using two-dimensional radiative transfer. Since scale coupling is inhibited in "pixels," in reality areas associated with

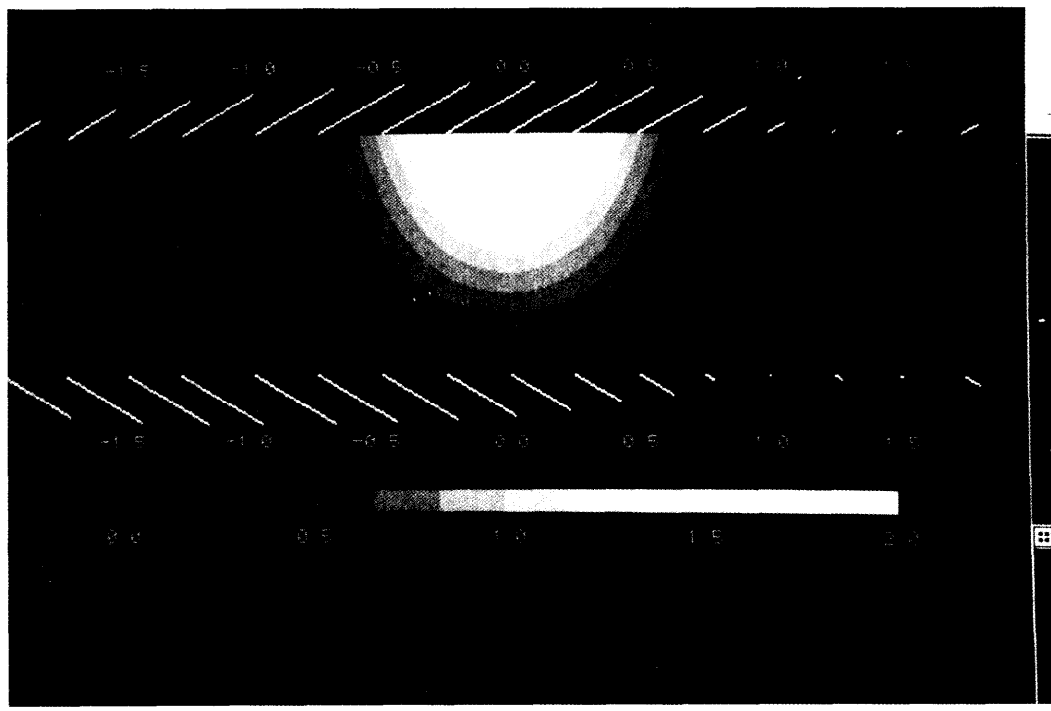

FIG. 9b. This image relates cloud extinction density to the cloud radiances exiting at the cloud boundaries. The length and direction of the processes emerging from the cloud are intended to illustrate the relative magnitudes of the radiances. The source (not shown) is located on the top right-hand side of the image, inclined 30° relative to a vertical axis. The extinction function and optical properties of the medium are as specified in Fig. 5a. The image shows that the radiance is not zero where the vertical optical thickness is minimum (in this case $\tau_{min} = 0.0$ at $x = -1.0$), as would be predicted by the independent pixel approximation. This is because of the reflection of the incident irradiance by the walls of the cloud. Thus, even when absorption is high ($\omega = 0.9$), the effects of cloud structure can still be important.

some assumed fixed scale, then energy balance calculations founded on such an assumption can have large errors whose magnitudes cannot be estimated.

This study has been intentionally limited to clouds of modest internal variability in order to acquire some understanding of the effects exerted by cloud structure

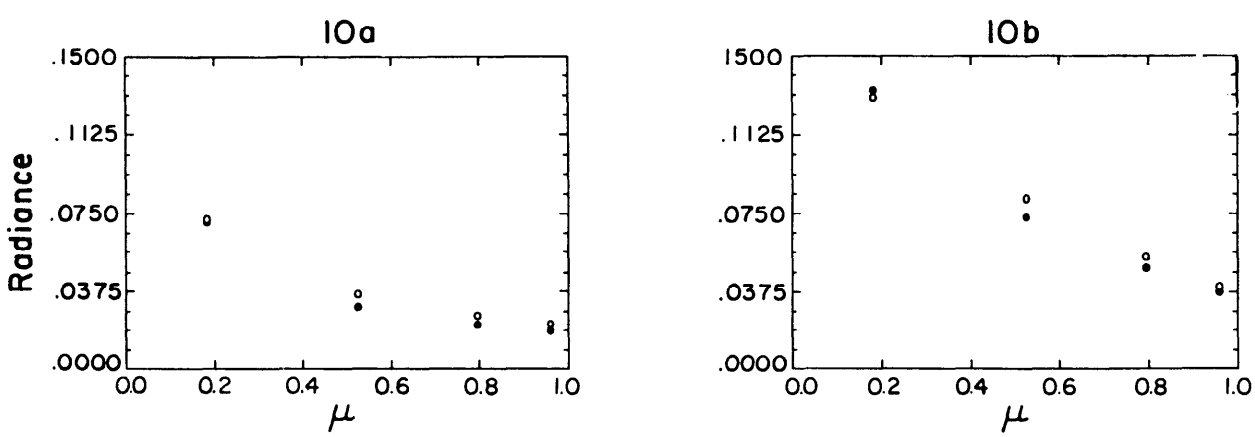

FIG. 10a. Domain-averaged radiances exiting the top boundaries of a cloud having extinction density, optical properties, and angle of illumination as given by Fig. 4a. The domain-averaged radiance is compared to that obtained by using the mean optical depth, in this case $\langle \tau \rangle = 0.25$ in a plane-parallel calculation employing the same phase function, illumination angle, and quadrature points. (b) Domain-averaged radiances exiting the top boundaries of a cloud having extinction density optical properties and angle of illumination as given by Fig. 5a. The domain-averaged radiance is compared to that obtained by using the mean optical depth, in this case $\langle \tau \rangle = 1.00$ in a plane-parallel calculation employing the same phase function, illumination angle, and quadrature points.

on the emerging radiation fields. The extremely different radiation fields associated with the different cloud structures as calculated in this study point to a need for a different way of thinking about the cloud radiation problem. The different cloud distributions used in this work can be thought of as instances or realizations generated by some probabilistic process.

The great spatial and temporal variability that characterizes naturally occurring clouds suggests that, at least for climatological studies, a stochastic approach to the radiation problem be pursued. In such a framework, the question is not what is the (deterministic) radiance or flux field given an extinction or scattering function but, rather, what are the statistical moments of the radiances and fluxes given the probabilistic process that generates extinction and scattering distributions. This kind of an approach has the virtue of characterizing uncertainties in the radiation field produced by cloud fluctuations, as well as fusing in situ observations of clouds with stochastic cloud modeling.

Acknowledgments. This work was supported by the Department of Energy (DE-FG02-90ER61067 and DE-A105-90ER61069), Brookhaven National Laboratories (466535), and the Office of Naval Research (N00014-91-J-1422, P00002). One of us (SCT) wishes to thank Dr. W. J. Wiscombe at NASA Goddard Space Flight Center for his support of this project. We also thank Drs. F. Evans and P. Flatau for useful discussions as well as the constructive criticisms of the reviewers. Computer calculations were carried out at Lawrence Livermore Laboratories, NCAR, and GSFC.

APPENDIX

Properties of the Fourier–Riccati Method

Whereas a common feature of solving most BVPs is to first discretize and then possibly transform the discrete system to resolve stability issues, the method described here first transforms ordinary differential equations (ODEs) and then performs a discretization. The hope is that the transformed system of ODEs is such that the IVPs are stable (a system is called stable is small changes in the input data produce small changes in the solution) and hence can be efficiently integrated. However, before discussing the numerical solution of (5), it is useful to know under what conditions those equations actually yield a solution of the two-point BVP represented by (1). It is also desirable to link the particular Riccati formulation used in this paper with established Riccati methods used to solve ODEs.

a. Solutions of the Fourier–Riccati Method

The issue of solutions can be addressed via the superposition principle. The solution $\tilde{\mathfrak{R}}(z)$ for the radiances at any point z can be expressed as a linear combination of the fundamental solution matrix ϕ, described by (10), and the particular solution $\mathbf{v}(z)$:

$$\begin{bmatrix} N^+(z) \\ N^-(z) \end{bmatrix} = \begin{pmatrix} \phi_{11}(z,0) & \phi_{12}(z,b) \\ \phi_{21}(z,0) & \phi_{22}(z,b) \end{pmatrix} \begin{bmatrix} s^+ \\ s^- \end{bmatrix} + \begin{bmatrix} v^+(z) \\ v^-(z) \end{bmatrix}, \tag{A1}$$

where $v^+(z)$ and $v^-(z)$ are components of the radiance vector $\mathbf{v}(z)$ identified with the solution to the initial value problem

$$\frac{d\mathbf{v}(z)}{dz} = \mathbf{A}(z)\mathbf{v}(z) + \tilde{\mathfrak{R}}_s(z) \tag{A2}$$

whose initial conditions are to be determined. The system transfer matrix, $\mathbf{A}(z)$, is given in (10), and vector $\tilde{\mathfrak{R}}_s(z)$, the vector describing the source function, by (9).

The boundary conditions s^+ and s^- are obtained by inverting (A1) to obtain

$$\begin{aligned} s^- &= \phi_{22}(z,b)^{-1}N^-(z) - \phi_{22}(z,b)^{-1}\phi_{21}(z,0)s^+ \\ &\quad - \phi_{22}(z,b)^{-1}v^-(z) \\ s^+ &= \phi_{11}(z,0)^{-1}N^+(z) - \phi_{11}(z,0)^{-1}\phi_{12}(z,b)s^- \\ &\quad - \phi_{11}(z,0)^{-1}v^+(z). \end{aligned} \tag{A3}$$

Substituting these equations into (A1) yields

$$\begin{aligned} &N^+(z) \\ &\quad = \phi_{12}(z,b)\phi_{22}(z,b)^{-1}N^-(z) \\ &\qquad + (\phi_{11}(z,0) - \phi_{12}(z,b)\phi_{22}(z,b)^{-1}\phi_{21}(z,0))s^+ \\ &\qquad + v^+(z) - \phi_{12}(z,b)\phi_{22}(z,b)^{-1}v^-(z) \\ &N^-(z) \\ &\quad = \phi_{21}(z,0)\phi_{11}(z,0)^{-1}N^-(z) \\ &\qquad + (\phi_{22}(z,b) - \phi_{21}(z,0)\phi_{11}(z,0)^{-1}\phi_{12}(z,b))s^- \\ &\qquad + v^-(z) - \phi_{21}(z,0)\phi_{11}(z,0)^{-1}v^+(z). \end{aligned} \tag{A4}$$

The reflection, transmission, and source functions can be identified as

$$\begin{aligned} R(z,b) &= \phi_{12}(z,b)\phi_{22}(z,b)^{-1} \\ R(z,0) &= \phi_{21}(z,0)\phi_{11}(z,0)^{-1} \\ T(b,z) &= (\phi_{11}(z,0) - R(z,b)\phi_{21}(z,b)) \\ T(0,z) &= (\phi_{22}(z,b) - R(z,0)\phi_{12}(z)) \\ \epsilon(b,z) &= v^+(z) - R(z,b)v^-(z) \\ \epsilon(0,z) &= v^-(z) - R(z,0)v^+(z), \end{aligned} \tag{A5}$$

which can be proved by showing that (A4) reproduces the equations given by (5). For example, consider the left column in (A5). Writing (12) in full and using the relation,

$$\frac{dR(z,b)}{dz} = \left(-R(z,b)\frac{d\phi_{22}(z,b)}{dz} + \frac{d\phi_{12}(z,b)}{dz}\right) \times \phi_{22}(z,b)^{-1}, \quad \text{(A6)}$$

leads to the first Riccati equation in (5). The transmission matrix $T(b,z)$ can be written as

$$T(b,z) = (\phi_{11}(z,0) - R(z,b)\phi_{21}(z,0)). \quad \text{(A7)}$$

Proceeding as before, the second equation of (5) is reproduced. Next, the pseudosource term $\epsilon(b,z)$ in (A4) can be written as

$$\epsilon(b,z) = v^+(z) - R(z,b)v^-(z). \quad \text{(A8)}$$

Writing (A2) in full and using (A8) leads to the third equation of (5). It now remains to determine the constants s^+ and s^-. These may be found by using the relations given by (A3), now expressed as

$$N^+(z) = R(z,b)N^-(z) + T(b,z)s^+ + \epsilon(b,z)$$
$$N^-(z) = R(z,0)N^+(z) + T(0,z)s^- + \epsilon(0,z) \quad \text{(A9)}$$

and using the boundary conditions for $N^+(z)$ and $N^-(z)$. Applying the boundary conditions $N^+(z=b) = N^+(b)$ and $N^-(z=0) = N^-(0)$ and using initial conditions given by (7) yields

$$v^+(0) = \epsilon(b,0) \quad v^-(b) = \epsilon(0,b)$$
$$v^+(b) = 0 \quad v^-(0) = 0$$

$$\phi(0) = \begin{pmatrix} T(b,0) & R(0,b) \\ 0 & 1 \end{pmatrix} \text{ and}$$

$$\phi(b) = \begin{pmatrix} 1 & 0 \\ R(b,0) & T(0,b) \end{pmatrix}. \quad \text{(A10)}$$

Hence, the Fourier–Riccati formulation with the identifications of (A5) yields a solution to the RTE expressed by (11).

b. *Uniqueness and stability of the Fourier–Riccati method*

Having shown that the Riccati formulation yields a solution to (11) as well as connecting operators **R** and **T** to the fundamental solution $\phi(z)$, questions concerning uniqueness and stability of the system of IVPs given by equations (5) can now be addressed. In order for the solution to (11) to be unique (hence allow for the unique solution of **R**, **T**, and ϵ), it is necessary that the matrix defined by $\mathbf{M}_u\phi(b) + \mathbf{M}_d\phi(0)$ be invertible. Although this proof is given in Ascher et al. (1988), it is readily demonstrated that this must be the case by applying the boundary conditions to Eq. (A1). The boundary conditions can be expressed as

$$\mathbf{M}_u\tilde{\mathfrak{R}}(b) + \mathbf{M}_d\tilde{\mathfrak{R}}(0) = \begin{bmatrix} N^+(b) \\ N^-(0) \end{bmatrix}. \quad \text{(A11)}$$

Inserting (A1) into (A11) yields

$$[\mathbf{M}_u\phi(b) + \mathbf{M}_d\phi(0)]\begin{bmatrix} s^+ \\ s^- \end{bmatrix} = \begin{bmatrix} N^+(b) \\ N^-(0) \end{bmatrix} - \mathbf{M}_u\mathbf{v}(b) - \mathbf{M}_d\mathbf{v}(0). \quad \text{(A12)}$$

Carrying out the indicated operations and using (A10) shows that $\mathbf{M}_u\phi(b) + \mathbf{M}_d\phi(0)$ is nonsingular, assuring that (11) possesses a unique solution.

The developments above are significant in describing the stability of the BVPs given by Eq. (3). It was remarked in section 3 that in the case of a medium exhibiting vertically uniform, horizontally variable extinction and scattering functions, that the fundamental solution was described by a (complex) matrix exponential. The stability of the solution is known in this case to depend on the sign of the eigenvalues of **A** [if all the eigenvalues are negative, **A** is called a stability matrix (Bellman 1970)]. Therefore, the solution $\tilde{\mathfrak{R}}(z)$ contains, in general, linear combinations of exponentials containing both positive and negative eigenvalues. For large z, the growing exponentials will dominate, and careless use of the fundamental solution leads to numerical instability. The behavior just described is called dichotomic, and is well known in the mathematical literature (Russell 1985; van Loon 1985; Mattheij 1985; Smith 1987). When the cloud also exhibits vertical nonuniformity, the eigenvalues of $\mathbf{A}(z)$ do not always characterize the stability of the BVP.

The Riccati approach is useful numerically because it decomposes $\phi(z)$ into a product of a direction matrix $\mathcal{T}(z)$ and a growth vector $\mathbf{w}(z)$. More specifically, $\phi(z)$ describes the propagation of the boundary conditions and $\mathcal{T}(z)$ consists of column vectors associated with the eigenvectors of $\mathbf{A}(z)$ in the constant coefficient case [in the variable coefficient case the interpretation is not so straightforward, but the notion of directional dependence is still applicable; see Ascher et al. (1988)]. Through $\mathbf{w}(z)$, the increasing and decaying solutions associated with (A2) are characterized. Through this function, stable computation of increasing solutions with decreasing distances and decaying solutions for increasing distances is possible. In the case of separated boundary conditions, or interest here, it can be shown that the initial condition at $z = 0$ controls the decaying solutions, whereas the condition at $z = b$ controls the increasing solutions of $\phi(z)$ (Dieci et al. 1988; Ascher et al. 1988).

To fix these ideas, transformation matrix $\mathcal{T}(z)$ is defined as

$$\mathcal{T}(z) = \begin{pmatrix} \mathbf{I} & \mathbf{0} \\ \mathbf{R}(z) & \mathbf{I} \end{pmatrix},$$

$$\text{and} \quad \mathcal{T}^{-1}(z) = \begin{pmatrix} \mathbf{I} & \mathbf{0} \\ -\mathbf{R}(z) & \mathbf{I} \end{pmatrix}; \quad \text{(A13)}$$

$\mathbf{R}(z)$ an $m \times m$ matrix (identified with the reflection matrix operator), and $\mathbf{I}$ a unit matrix also of size $m \times m$. Next, the following products:

$$\tilde{\mathbf{x}}(z) = \mathcal{T}(z)\mathbf{w}(z) \text{ and } \mathbf{w}_\epsilon(z) = \mathcal{T}^{-1}(z)\tilde{\mathbf{x}}_\epsilon(z) \quad \text{(A14)}$$

are formed, where

$$\mathbf{w}(z) = \begin{bmatrix} w(z)^+ \\ w(z)^- \end{bmatrix}.$$

It is readily seen that $\mathbf{w}(z)$ satisfies the relation

$$\frac{d\mathbf{w}(z)}{dt} = \mathbf{U}(z)\mathbf{w}(z) + \mathbf{w}_\epsilon(z). \quad \text{(A15)}$$

Matrix $\mathbf{U}(z)$ may also be shown to satisfy the Lyapunov equation

$$\mathbf{U}(z) = \mathcal{T}^{-1}(z)\left(A(z)\mathcal{T}(z) - \frac{d\mathcal{T}(z)}{dz}\right). \quad \text{(A16)}$$

Using (28,10) and *requiring* that $U(z)$ be upper triangular leads to

$$\begin{pmatrix} U_{11}(z) & U_{22}(z) \\ U_{21}(z) & U_{22}(z) \end{pmatrix} = \begin{pmatrix} -\mathbf{t}(z) + \mathbf{r}(z)\mathbf{R}(z) & \mathbf{r}(z) \\ \mathbf{0} & \mathbf{t}(z) - \mathbf{R}(z)\mathbf{r}(z) \end{pmatrix}$$

$$= \begin{pmatrix} -\mathbf{t}(z) + \mathbf{r}(z)\mathbf{R}(z) & \mathbf{r}(z) \\ -\mathbf{r}(z) + \mathbf{t}(z)\mathbf{R}(z) + \mathbf{R}(z)\mathbf{t}(z) - \mathbf{R}(z)\mathbf{r}(z)\mathbf{R}(z) - \dfrac{d\mathbf{R}(z)}{dz} & \mathbf{t}(z) - \mathbf{R}(z)\mathbf{r}(z) \end{pmatrix}, \quad \text{(A17)}$$

whence the Riccati equation is again recovered. The equations for the radiances are obtained using (A15)

$$\frac{dw^+(z)}{dz} = -(\mathbf{t}(z) - \mathbf{r}(z)\mathbf{R}(z))w^+(z) + \mathbf{r}(z)w^-(z) + w_\epsilon^+(z)$$

$$\frac{dw^-(z)}{dz} = (\mathbf{t}(z) - \mathbf{r}(z)\mathbf{R}(z))w^-(z) + w_\epsilon^-(z). \quad \text{(A18)}$$

The second of these equations is identical to that defining $\epsilon(0, z)$, the first to $v^+(z)$. Hence, the stability of the IVPs associated with (5) is established.

While (A18) can be stably integrated, there appears to be no guarantee that $\mathbf{R}(z)$ is bounded in the interval $(0, b)$. This can happen because the fundamental solutions $\phi_{22}(z, b)$ or $\phi_{11}(z, 0)$ may become singular. In that case, it is still possible to use the Riccati equation, provided that the integration at the trouble spot is restarted with a new and bounded value of $R(z)$. This corresponds to calculating a new fundamental solution on the next subinterval. The exact details for carrying out this procedure are discussed at length in Ascher et al. (1988) and will not be elaborated here. Another technique that has been successfully employed to continue the integration of the Riccati equation is the use of $\mathbf{R}^{-1}$ (see Scott and Vandevender 1975). It can be shown that the inverse also satisfies a Riccati equation, with a starting value taken just prior to reaching the singularity. This method has received criticism from Nelson et al. (1978).

c. *Boundedness of the Fourier–Riccati solutions*

The results obtained above are in a sense overly general: if the RTE is to have a solution within any interval $(0, b)$ then $\mathbf{R}$ *must* possess certain properties that prevent the potentially unbounded growth of $\mathbf{R}$ described in the previous paragraph. Certainly in practice, no great difficulties were encountered in integrating (5) for any reasonably behaved scattering and extinction functions. Then the integrability of the Riccati equations depends crucially on the local transmission and scattering operators $\mathbf{t}$ and $\mathbf{r}$, which have not yet been discussed.

Confining the discussion of radiative transfer to two dimensions for simplicity of exposition but without loss of generality, and noting that the sinusoidal components of the radiance vector are all equal to zero because the radiance vector is symmetric in azimuth, the structure of the aforementioned matrices is now described. The transmission matrix exhibits the following structure,

$$\mathbf{t} = \mathbf{t}_\alpha + \mathbf{t}_v - \mathbf{t}_s, \quad \text{(A19)}$$

where $\mathbf{t}_\alpha$ is (in this example, only two azimuthal modes $M = 2$ are needed to show the pattern in the matrix)

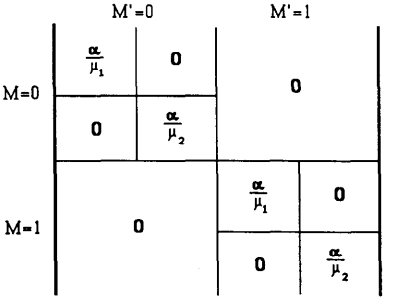

(A20)

and α is

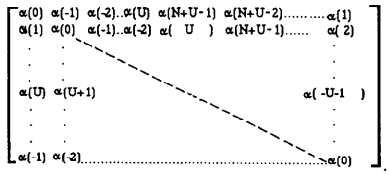

. (A21)

Matrix α, a circulant matrix, is written in full. Each of its elements $\alpha(k)$ contains amplitude and phase information associated with the Fourier transform of the extinction function. The dependence of $\alpha(k)$ on the vertical position z has been suppressed for notational convenience. This matrix circulant character arises as a consequence of the periodicity imposed by the discrete Fourier transform ($\alpha(i + mT) = \alpha(i)$ for any integer m) and is defined by the spatial convolution of the extinction with the radiance in (1).

Matrix $\mathbf{t}_v$ has purely imaginary elements and arises from two operations: azimuthal integration of the radiance followed by Fourier transformation of the horizontal gradient. Its structure is (in this example the form of the matrix is illustrated with three azimuthal modes):

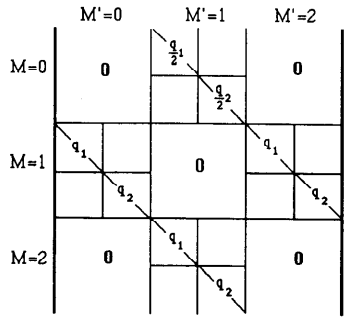

, (A22)

where $\mathbf{q}_k$ is a vector in u whose elements are

$$\frac{i\pi\eta_k}{L_x\mu_k}[-U \ldots U-1]. \tag{A23}$$

The index k refers to the kth quadrature point and $2L_x$ is the horizontal spatial domain spanned by the cloudy medium. Matrix $\mathbf{t}_s$ is given by

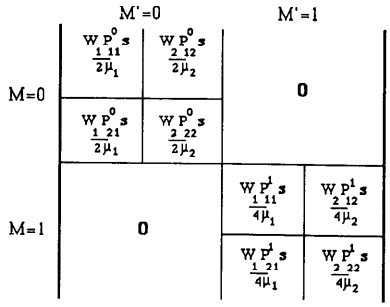

, (A24)

whereas matrix $\mathbf{r}$ is structurally identical in form to $\mathbf{t}_s$ differing only by the replacement of the moments of the phase function P_{ij}^n by P_{-ij}^n. Quantities W_k and s appearing in the matrix subblocks designate the weights associated with the (Gaussian) quadrature points and the circulant matrix associated with the scattering function, patterned after the extinction matrix, respectively.

The connection between the boundedness of the Riccati equation and energy conservation has been thoroughly investigated by Bellman et al. (1965) and Bellman (1970). In those works the fundamental properties of $\mathbf{R}$ and $\mathbf{T}$ are established for a scattering and absorbing medium whose inhomogeneity is confined to variations along the z axis only. Furthermore, the Riccati equations are derived in physical space, hence the elements of the local reflection and transmission matrices are purely real quantities. More precisely, $r_{ij} \geq 0$ while $\mathbf{t}$ is a nonnegative matrix. This contrasts with the properties of the matrix operators in this study, which are in general complex. Hence, the results of those studies are unfortunately not immediately applicable to the Riccati formulation developed in this paper in spite of the formal similarity of the Riccati equations. Therefore, a generalization of the developments of Bellman et al. (1965) appears necessary. Instead of pursuing such an extension here whose development warrants separate study, some aspects of the numerical behavior of the Riccati equation will be described. These observations are evidence supporting the conjecture that the latter system remains bounded over the interval of integration. Beginning with the Riccati equation

$$\frac{d\mathbf{R}(z,0)}{dz} + \mathbf{R}(z,0)\mathbf{r}\mathbf{R}(z,0) - \mathbf{R}(z,0)\mathbf{t} - \mathbf{t}\mathbf{R}(z,0) + \mathbf{r} = 0 \tag{A25}$$

and focusing on a vertically uniform, horizontally inhomogeneous medium, let the analytical solution be given by

$$\mathbf{R}(z,0) = e^{-tz}\psi e^{-tz}. \tag{A26}$$

Such a transformation leads to the integral equation

$$\mathbf{R}(t,0) = -\int_0^t e^{\mathbf{t}(z-z')}(\mathbf{R}(z',0)\mathbf{r}\mathbf{R}(z',0) + \mathbf{r}) \times e^{\mathbf{t}(z-z')}dz', \tag{A27}$$

as is easily verified. If this integral is to remain bounded over some specified interval, it is reasonable to expect the complex eigenvalues λ_k of $\mathbf{t}$ to have a positive real part greater than zero. This implies that $R(z)$ is decreasing exponentially with increasing distance z. Therefore, the previous integral equation can be written as

TABLE A1. This table summarizes the numerical behavior of the eigenvalues associated with the t matrix. In all cases the eigenvalues were positive. With the exception of the plane-parallel case, degeneracy (denoted by D) was observed in isotropic nonconservative scattering. It is interesting that no degeneracy (N) was noted in conservative scattering with an anisotropic phase function. The eigenvalues were calculated to within seven decimal places of precision. Symbol H.G designated a Henyey–Greenstein-type phase function. Phase C.1 is the standard Deirmendjian phase function.

α	s	Phase H.G		Phase C.1	
1	1	$g = 0.0$	D	—	
		$g = 0.7$	D	—	
$\exp(-\pi x^2)$	$\exp(-\pi x^2)$	$g = 0.0$	D	$g = 0.$	N
		$g = 0.7$	N		
$1 + \sin(\pi x)$	$1 + \sin(\pi x)$	$g = 0.0$	D	$g = 0.$	N
		$g = 0.7$	N		
2	$1 + \sin(-\pi x)$	$g = 0.0$	D	$g = 0.$	D
		$g = 0.7$	D		
1	$\exp(-\pi x^2)$	$g = 0.0$	D	$g = 0.$	D
		$g = 0.7$	D		

$$\mathbf{R}_{n+1} = -\int_0^t e^{\mathbf{t}(z-z')}(\mathbf{R}_n\mathbf{r}\mathbf{R}_n + \mathbf{r})e^{\mathbf{t}(z-z')}dz' \quad \text{(A28)}$$

with $\mathbf{R}_0 = 0$. Hence, $\mathbf{R}_n$ should constitute a sequence of successive approximations converging in the limit of infinite iteration to $\mathbf{R}$. The necessity of having positive eigenvalues is that diagonalizing $e^{-\mathbf{t}z}$ results in a matrix whose entries are linear combinations of $z^{r-1}e^{-\lambda_k z}$, the exponent r being determined by the multiplicity of the kth eigenvalue. The Jordan canonical form that generates the aforementioned linear combination of exponentials collapses to a diagonal matrix if and only if all the eigenvalues are distinct. Surprisingly, numerical experiments have shown that it is possible for all the λ_k to be different. The relationship of λ_k to the extinction, scattering and phase functions is not simple, as is evident from Table A1.

REFERENCES

Aida, M., 1977: Scattering of solar radiation as a function of cloud dimensions and orientation. *J. Quant. Spectrosc. Radiat. Transfer,* **17,** 303–310.

Ascher, U. M., R. M. M. Mattheij, and R. D. Russell, 1988: *Numerical Solution of Boundary Value Problems for Ordinary Differential Equations.* Prentice Hall Series in Computational Mathematics, 595 pp.

Avaste, O. A., and G. M. Vaynikko, 1974: Solar radiation transfer in broken clouds. *Izv. Atmos. and Oceanic Phys.,* **10,** 1054–1061.

Barkstrom, B. R., and R. F. Arduini, 1977: The effect of finite size of clouds upon the visual albedo of the earth. *Radiation in the Atmosphere,* H. J. Bolle, Ed., Science Press, 88-190.

Barnett, S., 1984: *Matrices in Control Theory.* R. E. Krieger, 192 pp.

Bellman, R., 1970: *Introduction to Matrix Analysis.* 2d ed. McGraw Hill, 403 pp.

——, K. L. Cooke, R. Kalaba, and G. M. Wing, 1965: Existence and uniqueness theorems in invariant imbedding—I. Conservation principles. *J. Math. Anal. Appl.,* **10,** 234–244.

Busygin, V. P., N. A. Yevstatov, and E. M. Feigelson, 1973: Optical properties of cumulus clouds and radiant fluxes for cumulus cloud cover. *Izv. Atmos. Oceanic Phys.,* **10,** 1142–1151.

——, ——, and ——, 1977: Calculation of the direct, scattered and total solar radiant fluxes and their distributions for cumulus clouds. *Izv. Atmos. Oceanic Phys.,* **13,** 184–190.

Cahalan, R. F., 1989: Overview of fractal clouds. *Advances in Remote Sensing Retrieval Methods.* A. Deepak, H. E. Fleming, and J. S. Theon, Eds., A. Deepak, 371–389.

——, and J. H. Joseph, 1989: Fractal statistics of cloud fields. *Mon. Wea. Rev.,* **117,** 261–272.

Cogley, A. C., 1981: Initial results for multidimensional radiative transfer by the adding/doubling method. *Fourth Conf. on Atmospheric Radiation,* Toronto, Amer. Meteor. Soc., 79–81.

Crosbie, A. L., and T. L. Linsenhardt, 1978: Two-dimensional isotropic scattering in a semi-infinite medium. *J. Quant. Spectrosc. Radiat. Transfer,* **19,** 257–284.

Davies, R., 1976: The three-dimensional transfer of solar radiation in clouds. Ph.D thesis, University of Wisconsin, 219 pp. [Available from Dept. of Atmospheric and Oceanic Sciences, 1225 West Dayton St., Wisconsin 53706.]

——, 1978: The effect of finite geometry on three-dimensional transfer of solar irradiance in clouds. *J. Atmos. Sci.,* **35,** 1712–1724.

——, 1984: Reflected solar radiances from broken cloud scenes and the interpretation of scanner measurements. *J. Geophys. Res.,* **89,** 1259–1266.

Davis, A., S. Lovejoy, and D. Schertzer, 1991: Discrete angle radiative transfer in a multifractal medium. *SPIE Proc.,* 1558.

——, P. Gabriel, S. Lovejoy, D. Schertzer, and G. L. Austin, 1990: Discrete angle radiative transfer 3. Numerical results and meteorological applications. *J. Geophys. Res.,* **95,** 11 729–11 742.

Derr, V., and R. Gunter, 1982: EPOCS 1980: Summary data report—Aircraft measurements of radiation, turbulent transport and profiles in the atmospheric and oceanic boundary layers of the tropical eastern Pacific. NOAA Tech. Memo. ERL WPL-101, NOAA Wave Propagation Lab, Boulder, CO.

Dieci, L., M. R. Osborne, and R. D. Russell, 1988: A Riccati transformation method for solving linear BVs. I: Theoretical aspects. *SIAM J. Numer. Anal.,* **25,** 1055–1092.

Diner, D. J., and J. V. Martonchik, 1984: Atmospheric transfer of radiation above an inhomogeneous non-Lambertian reflective ground—II. Computational considerations and results. *J. Quant. Spectrosc. Radiat. Transfer,* **32,** 279–304.

Evans, K., 1992: Two-dimensional radiative transfer in cloudy atmospheres. The spherical harmonic spatial grid method. *J. Atmos. Sci.,* **50,** 3111–3124.

Flatau, J. P., and G. L. Stephens, 1988: On the fundamental solution of the radiative transfer equation. *J. Geophys. Res.,* **93,** 11 037–11 050.

Gabriel, P., S. Lovejoy, A. Davis, D. Schertzer, and G. L. Austin, 1990b: Discrete angle radiative transfer 2. Renormalization approach for homogeneous and fractal media. *J. Geophys. Res.,* **95,** 11 717–11 728.

Gantmacher, F. R., 1959: *Applications of the Theory of Matrices.* Wiley-Interscience, 317 pp.

Gilbert, F., and G. E. Backus, 1966: Propagator matrices in elastic wave and vibration problems. *Geophys.,* **31,** 326–332.

Glazov, G. N., and G. A. Titov, 1979: Average solar radiation fluxes and angular distribution in broken clouds. *Izv. Atmos. Oceanic Phys.,* **15,** 802–806.

Grant, I. P., and G. E. Hunt, 1969a: Discrete space theory of radiative transfer, I. Fundamentals. *Proc. Roy. Soc. London,* **313,** 183–197.

——, and ——, 1969b: Discrete space theory of radiative transfer, II. Stability and non-negativity. *Proc. Roy. Soc. London,* **313,** 199–216.

Harnad, J., P. Winternitz, and R. L. Anderson, 1983: Superposition principles for matrix Riccati equations. *J. Math. Phys.,* **24,** 1062–1072.

Karp, A. H., J. Greenstadt, and J. A. Filmore, 1980: Radiative transfer through an arbitrarily thick, scattering atmosphere. *J. Quant. Spectrosc. Radiat. Transfer,* **24,** 391–406.

Kattawar, W. G., and B. J. Thompson, 1991: *Selected Papers on Multiple Scattering in Plane Parallel Atmospheres and Oceans:*

Methods. George W. Kattawar and Brian J. Thompson, Eds., SPIE Milestone Series, Vol. MS42, SPIE Optical Engineering Press, 642 pp.

King, W. D., C. T. Maher, and G. A. Hepburn, 1981: Further performance tests on the CSIRO liquid water probe. *J. Atmos. Sci.*, **38,** 195–200.

Kobayashi, T., 1991: Reflected solar flux for horizontally inhomogeneous atmospheres. *J. Atmos. Sci.*, **48,** 2436–2447.

Kuo, K. S., R. M. Welch, and S. K. Sengupta, 1988: Structural and textural characteristics of cirrus clouds observed using high spatial resolution Landsat imagery. *J. Appl. Meteor.*, **27,** 1242–1248.

Lovejoy, S., 1982: Area-perimeter relation for rain and cloud areas. *Science*, **216,** 185–187.

——, A. Davis, P. Gabriel, D. Schertzer, and G. L. Austin, 1990: Discrete angle radiative transfer 1. Scaling and similarity, universality and diffusion. *J. Geophys. Res.*, **95,** 11 699–11 715.

McKee, T. B., and J. T. Cox, 1974: Scattering of visible light by finite clouds. *J. Atmos. Sci.*, **31,** 1885–1892.

Mattheij, R. M. M., 1985: Decoupling and stability of algorithms for boundary value problems. *SIAM Rev.*, **27,** 1–44.

Mironova, L. M., 1983: Scattering of light by a horizontally inhomogeneous cloud. *Izv. Atmos. and Oceanic Phys.*, **19,** 449–454.

Nelson, P., A. K. Ray, and G. M. Wing, 1978: On the effectiveness of the inverse Riccati transformation in the matrix case. *J. Math. Anal. Appl.*, **65,** 201–210.

O'Brien, D. M., 1992: Accelerated quasi Monte Carlo integration of the radiative transfer equation. *J. Quant. Spectrosc. Radiat. Transfer*, **48,** 41–59.

Preisendorfer, R. W., and G. L. Stephens, 1984: Multimode radiative transfer in finite optical media, 1: Fundamentals. *J. Atmos. Sci.*, **41,** 709–724.

Press, H. W., B. P. Flannery, S. A. Teukolsky, and W. T. Vetterling, 1988: *Numerical Recipes*. Cambridge University Press, 702 pp.

Rand, D. W., and P. Winternitz, 1984: Nonlinear superposition principles: A new numerical method for solving matrix Riccati equations. *Comp. Phys. Commun.*, **33,** 305–328.

Rhys, F. S., and A. Waldvogel, 1986: Fractal shape of hail clouds. *Phys. Rev. Lett.*, **56,** 784–787.

Romanova, L. M., 1975: Radiation transfer in a horizontally inhomogeneous scattering medium. *Izv. Atmos. and Oceanic Phys.*, **11,** 808–818.

——, 1976: Invariance principles for horizontally inhomogeneous turbid media. *Izv. Atmos. and Oceanic Phys.*, **12,** 820–833.

——, 1978: Applying the perturbation method to the problem of the passage of light through a horizontally inhomogeneous cloud. *Izv. Atmos. Oceanic Phys.*, **14,** 889–895.

——, 1985: Radiation density and absorption in homogeneous and horizontally inhomogeneous clouds. *Izv. Atmos. Oceanic Phys.*, **21,** 642–648.

——, and I. M. Tarabukhina, 1981: Light reflection by a sunlit horizontally inhomogeneous cloud. *Izv. Atmos. and Oceanic Phys.*, **17,** 19–26.

Russell, R., 1985: A unified view of some recent developments in numerical solution of BVODES. *Progress in Scientific Computing, Numerical Boundary Value ODEs, Proc. Int. Workshop*, U. M. Ascher and R. Russell., Eds., Birkhauser, 1–19.

Scott, M. R., and W. H. Vandevender, 1975: A comparison of several invariant imbedding algorithms for the solution of two-point boundary value problems. *Appl. Math. Comput. I.*, **3,** 187–218.

Smith, D. R., 1987: Decoupling and order reduction via Riccati transformation. *SIAM Rev.*, **29,** 91–113.

Stamnes, K., 1988: Numerically stable algorithm for discrete ordinates method radiative transfer in multiple scattering and emitting layered media. *Appl. Opt.*, **27,** 2502–2509.

Stephens, G. L., 1986: Radiative transfer in spatially heterogeneous, two-dimensional, anisotropically scattering media. *J. Quant. Spectrosc. Radiat. Transfer*, **36,** 51–67.

——, 1988: Radiative transfer through arbitrarily shaped optical media. Part I: A general model of solution. *J. Atmos. Sci.*, **45,** 1818–1836.

——, 1988: Radiative transfer through arbitrarily shaped optical media. Part II: Group theory and simple closures. *J. Atmos. Sci.*, **45,** 1837–1848.

——, and R. W. Preisendorfer, 1984: Multimode radiative transfer in finite optical media, 2: Solutions. *J. Atmos. Sci.*, **41,** 725–735.

Titov, G. A., 1979: Solar Radiation transfer modeling for cumulus cloud conditions. *Izv. Atmos. Oceanic Phys.*, **15,** 432–436.

——, 1980: Statistical characteristics of short wavelength solar radiation in the presence of cumulus cloudiness. *Izv. Atmos. Oceanic Phys.*, **16,** 500–505.

Tsay, S., and K. Jayaweera, 1984: Characteristics of arctic stratus clouds. *J. Atmos. Sci.*, **41,** 1336–1355.

Twomey, S., and T. Cocks, 1980: Spectral reflectance of clouds in the near-infrared: Comparison of measurements and calculations. *J. Meteor. Soc. Japan*, **60,** 583–592.

——, and K. J. Seton, 1980: Inferences of gross microphysical properties of clouds from spectral reflectance measurements. *J. Atmos. Sci.*, **37,** 1065–1069.

Van de Hulst, H. C., 1963: A new look at multiple scattering. Tech. Rep. Goddard Institute for Space Studies, NASA, 91 pp.

van Loon, P., 1985: Riccati transformation: When and how to use? Numerical Solution of BVODES. *Progress in Scientific Computing, Numerical Boundary Value ODEs., Proc. Int. Workshop*, U. M. Ascher and R. Russell, Eds., Birkhauser.

Welch, R. M., and W. G. Zdunkowski, 1981: The effect of cloud shape on radiative characteristics. *Contrib. Atmos. Phys.*, **54,** 258–272.

——, K. S. Kuo, B. A. Wielicki, S. K. Sengupta, and L. Parker, 1988a: Marine stratocumulus cloud fields off the coast of southern California observed by Landsat imagery. 1, Structural characteristics. *J. Appl. Meteor.*, **27,** 341–362.

——, S. K. Sengupta, and K. S. Kuo, 1988b: Marine stratocumulus cloud fields off the coast of Southern California observed by Landsat imagery. 1, Textural analysis. *J. Appl. Meteor.*, **27,** 341–362.

Wielicki, A. B., and R. M. Welch, 1986: Cumulus cloud properties derived using Landsat satellite data. *J. Climate Appl. Meteor.*, **25,** 261–276.

Wing, G. M., 1962: *An Introduction to Transport Theory*. Wiley-Interscience, 165 pp.

Wiscombe, W. J., 1983: Atmospheric Radiation: 1975–1983. *Rev. Geophys. Space Phys.*, **21,** 997–1021.

——, R. M. Welch, and W. D. Hall, 1984: The effects of very large drops on cloud absorption. Part 1: Parcel models. *J. Atmos. Sci.*, **41,** 1336–1355.

Yano, J. I., and Y. Takeuchi, 1990: Fractal dimension analysis of horizontal cloud pattern in the intertropical convergence zone. *Scaling, Fractals, and Non-linear Variability in Geophysics*, D. Schertzer and S. Lovejoy, Eds., Kluwer.